

©Copyright 2022

Mareldi Ahumada-Parás

Resilience in Multi-Energy Systems

Mareldi Ahumada-Parás

A dissertation
submitted in partial fulfilment of the
requirements for the degree of

Doctor of Philosophy

University of Washington

2022

Reading Committee:

Daniel Kirschen, Chair

Baosen Zhang

Miguel A. Ortega-Vazquez

Program Authorized to Offer Degree:

Electrical Engineering

University of Washington

Abstract

Resilience in Multi-Energy Systems

Mareldi Ahumada-Parás

Chair of the Supervisory Committee:
Donald W. and Ruth Mary Close Professor Daniel Kirschen
Electrical and Computer Engineering

This dissertation addresses power system planning strategies for resilience and the interaction with other critical infrastructures, in particular natural gas networks and health systems. In light of recent events, from a global pandemic to wildfires, hurricanes, earthquakes and freezing temperatures, there is an urgency to adapt our power grid's operation and planning in order to withstand and recover from the challenges posed by extreme events. Current practices, metrics and standards no longer meet our society's needs for more, reliable and resilient power. This work focuses on four main aspects of resilience: robustness, resourcefulness, recovery and adaptability. First, an evaluation of resourcefulness in the restoration phase after a natural disaster. We compared stand alone PV-battery system against emergency diesel generators to supply critical loads during an extended outage. Secondly, mapping interdependence of power and natural gas networks. We modeled both infrastructures and conducted N-k analyses to identify vulnerabilities of each system and the quantify the dependency of gas-fired generators on natural gas pipelines. Lastly, we focused on different investments strategies to increase robustness of the grid by comparing hardening actions against increasing distributed energy resources. Our findings in each project aid decision making as we plan for more resilient grids against natural disasters.

TABLE OF CONTENTS

	Page
List of Figures	iii
List of Tables	v
Glossary	vi
Chapter 1: Introduction	1
1.1 Motivation for Resilience	1
1.2 Resilience Framework	2
1.3 Scope of the Work and Organization	4
Chapter 2: Resourcefulness in Power Systems Post-Natural Disasters	7
2.1 Motivation	7
2.2 Puerto Rico after Hurricane Maria, a Comprehensive Case Study	9
2.3 Optimal PV-Battery Design	19
2.4 Simulation Results	23
2.5 Summary	25
Chapter 3: Joint Power-Natural Gas Infrastructure Framework for Analysis in Planning	30
3.1 Motivation	30
3.2 Gas Network Framework	33
3.3 Problem Formulation	35
3.3.1 Steady State Gas Flow Equations	37
3.3.2 Power Model	38
3.3.3 $N-k$ interdiction problem for Gas Network	39
3.3.4 Joint Power-Gas Network	40
3.3.5 Threat Model	40

3.4	Proposed Method	42
3.5	Results	46
3.5.1	Performance of the Cutting-Plane Algorithm	47
3.5.2	Gas-fired Generation Capacity Loss in the Power Grid	48
3.5.3	Joint Power and Natural Gas	49
3.5.4	Probabilistic Assessment of Natural Disaster	53
3.6	Summary	54
Chapter 4:	Evaluation of Robustness Strategies Against Extreme Events	56
4.1	Motivation	56
4.2	Literature Review	57
4.3	Proposed Method	59
4.4	Simulation Results	65
4.5	Summary	67
Chapter 5:	Conclusion	70
5.1	Key Results	70
5.2	Suggestions for Future Research	71
	Bibliography	73
Appendix A:	Topic Guide to conduct Interviews in Puerto Rico after Hurricane Maria	80
A.1	Topic Guide: Patients	80
Appendix B:	Relaxations for the MGS Problem	82
B.1	MINLP reformulation	82
B.2	MISOCP relaxation	83

LIST OF FIGURES

Figure Number	Page
1.1 NIAC Resilience Construct [10]	3
2.1 Restoration of power to customers in Puerto Rico after Hurricane Maria. Note the significant different between the San Juan urban area and the mountainous and directly hit region of Caguas. Based on data from [45].	10
2.2 Top view of a PV-battery system designed at the University of Washington. Note that the batteries, data logger and majority of the cables are inside the box.	15
2.3 Electrical load profiles of eight different households over one to three days.	17
2.4 Generation and consumption for 8 households during a 3 day period	18
2.5 Battery degradation studies: (a) number of battery cycles over 50% DoD and 50% or less DoD for six households; and (b) average daily battery temperature for six households over 105 days.	20
2.6 Scenario A: (a) the minimum battery capacity required to power critical loads over a year against the PV system size; and (b) total PV and battery cost against the PV system size.	27
2.7 Cost of using a diesel generator and PV-battery system after a disaster.	28
3.1 Power and natural gas network structures and the area impacted by a single natural disaster event.	41
3.2 Area defined by an epicenter C and a radius R that represents a given earthquake strength and location.	42
3.3 Belgian Network with interdicted components in worst case scenarios for $k = 1, 2, 3, 4$	47
3.4 Power Capacity Lost per generator for $\mathcal{A} = 100$. IEEE-14 case system	53
3.5 Gas not served for $\mathcal{A} =$ large, medium and small event magnitudes	54
4.1 Resilience Evaluation Model	60
4.2 Distribution network with random faults, hardened lines and installed distributed resources.	61

4.3	Measured wind speeds at 7 meteorological sites in Santiago, Chile	62
4.4	Line Fragility Curves for 3 line lengths.	63
4.5	normal and extreme wind event characterization	64
4.6	Binary component states for a base fragility curve (blue) and the hardened case (red).	65
4.7	Investment decomposition for Harding and DERs for different portfolio strategies. Size of the circles represents the LOLE.	67
4.8	LOLE vs Investment Cost with Low VoLL	68
4.9	LOLE vs Investment Cost with High VoLL	69

LIST OF TABLES

Table Number	Page
2.1 The maximum and average measured power, time-of-use and duration of critical electrical loads.	13
2.2 Summary of the systems installed.	16
2.3 Energy consumption details of the six households.	19
2.4 Comparison of various PV-battery system designs. The cost only consists of the PV and batteries and r is the number of battery replacements.	29
3.1 Belgian gas network results	49
3.2 New England gas network results	50
3.3 gaslib-582 results	50
3.4 Generation capacity loss for the Belgian-IEEE 14 network. During normal operation the power produced from all the gas-fired power plants is 39.67 MW	51
3.5 Generation capacity loss for the New England-IEEE 36 network. During normal operation the power produced from all the gas-fired power plants is 513.21 MW	51
3.6 Gas Shed and Lost Power Capacity per Damaged Area Size For Belgian-IEEE 14 Networks	52
3.7 Gas Shed and Lost Power Capacity per Damaged Area Size For NE-IEEE 36 Networks	53
A.1 Patients	81

GLOSSARY

HILP: High Impact Low Probability

LOLE: Loss of Load Expectation

DER: Distributed Energy Resources

DG: Distributed Generators

PV: Photo-Voltaic

SOC: State-of-Charge

COPD: Chronic Obstructive Pulmonary Disease

CPAP: Continuous Positive Airway Pressure

PEG: Percutaneous Endoscopic Gastronomy

MPPT: Maximum Power Point Tracking

DOD: Depth-of-Discharge

BMS: Battery Management Systems

COT: Continuous Operation Time

PDE: Partial Differential Equations

MGS: Minimal Gas Shedding

LIP: Linear Integer Programming

MINLP: Mixed-Integer Non-Linear Programming

MISOCP: Mixed-Integer Second-Order Cone Programming

ACKNOWLEDGMENTS

There are certainly many people throughout my life and education that made this thesis come to fruition. Going back as early as elementary school for a PhD acknowledgment section would sound a bit much for some, but in my case that was the moment I realized or rather was indoctrinated (no pun intended) by my parents that pursuing a PhD was in my future. All jokes aside, a goal that was set at a very young age would not have been possible without the tremendous help of everyone explicitly and implicitly mentioned in the next few paragraphs. In no particular order I will start writing from the bottom of my heart as I sit at my office desk at the University of Washington inspired by an amazing view I was lucky to have.

First and foremost thank you to my parents and brother. My father who always reminds me that I was lucky to be born in the circumstances that made it plausible to attain this degree and to always recognize that it is not the reality for many others. He has always pushed me to do better by others. My mother who maintains balance in the universe, at least in mine, by always being supportive and reminding me to take a breath and reflect. Thank you to my brother, who is the better version of me in every aspect, to his wisdom, support and for always being there, always. Thanks to my extended family, my main pillar in life.

I would like to thank my advisor, Professor Kirschen, for his patience and invaluable guidance as I discovered my way through the fascinating world of power systems. He supported me in all of my projects and permitted me to explore freely. Thank you to my mentors from the University of Washington, Miguel Ortega-Vazquez, for admitting me into the program and always providing great career advice. Baosen Zhang, for being part of all my milestones

and encouragement to become better researcher. To professors Richard Christie and Brian Johnson for their constructive feedback along the way.

Thank you to Professor Rodrigo Moreno who I had the fortune of collaborating with during my final year. I found his work most inspiring and I was lucky to have a mutual interest in resilience. Thank you to Russell Bent and Kaarthik Sundhar for their invaluable contribution to the fundamentals of my research. Furthermore, helping and supporting me through the most challenging time. Thank you to Professor Lilo Pozzo and Marvi Matos, both incredibly intelligent, driven and kind people that unknowingly motivated my whole research focus. I will be forever thankful for allowing me to learn passion for research, and what it means to care, impact for the better and be a leader in ones community. Our collaboration was in part made possible by the support from the Clean Energy Institute where I made some of the strongest networks for my research.

This thesis is a small fraction of the valuable lessons I gained at the REAL lab. I would like to thank the incredible people from my lab and the ECE department that enriched my research and helped me grow both technically and as a person. Yushi, for being an early mentor as I on-boarded my PhD. Ryan for being an excellent lab leader who always made sure everyone had everything they needed to succeed. To Daniel Olsen and Abeer for being the perfect office mates and teaching me to 'say no' and stand up for myself. Chanaka, for his friendship and who I was fortunate to embark with on many projects. Tinu for her enormous wisdom and reminding me to keep my eyes on the prize. Lane, who was my biggest ally in the lab. He motivated me to get to the finish-line. I will be forever grateful for his relentless effort to find me a post-doc and for always being accountable. Very special thanks to Nina for enlightening me. For her patience, motivation and unconditional support. She has thought me the definition of *resilient*. Gord, my research role-model who I hope to work for someday. To Rahul, Daniel Tabas, Jackie and Wenqi for adding livelihood to the lab. Lastly to the REAL alumni Greats Kelly, Ahlmahz, Anna, Yuanyuan, Yao, Trisha, Kelsey

for granting me the best support group as we all navigated the challenges of PhD life.

Form the ECE department, Momona, my first friend at UW who was essential in my well- being. Jordan, who I had the pleasure of being co-presidents with of our department student organization and for making ECE a better place. Diego, for helping me represent the Latinos in ECE. The most brilliant person in the department who helped our entire class understand Convex Optimization. Thank you to James, Brenda, Maneeshika, and many other who I had the fortune to have crossed paths with in the department.

This work would have not been possible without the sponsorship of Fulbright Garcia Robles, a complete honor to represent such an outstanding organization. Thank you to P.E.O. and the Seattle Chapters for making sure I could focus on my studies and never go without a cup of coffee. All the generous gift cards are the reason I started drinking coffee when I arrived to Seattle, so thank you (?).

Thanks to my international friends, Arbel, Marcela, Robbie, GB, Ana, Aline, Anik and Adiya, Vitalii, Ghada, Seemi, Danish, Huong, Mohammed, MG and Eric, Neto, Ceci and Fefo, Roque, Antonio, Kevin, Laura, Susana and Dani, Suny and Sheehan for giving me a home away from home. Thank you to Rossana and Alex, the best housemates ever. Watching sports on weekends with both of you was my favorite time in Seattle. Thank you to Yao, my PhD buddy from start to finish. He is my favorite triple crown Ph.D/Dr./Professor in the world.

My GE family Carlos, Ivan, Mikhail, Pepe, Leo and Paulina who helped me develop as an engineer, grow as a person, and had the best of times with. Lastly to my closest friend group back home that I can always count on for anything, Mafer, July, Alex, Pame, Ana, Luis, Emma, and Giovanna. Last eternal acknowledgement to Mariana, an unconditional friend, who has carried me through thick and thin, she is always there to make sure I can get by.

Thank you to all for your contributions in my work!

DEDICATION

to my parents Margarita and Ívico, and to my amazing brother Alonso.

Special dedication to Mabis, who guided my every step.

Chapter 1

INTRODUCTION

There's no such thing as bad weather, only unsuitable clothing.

- Alfred Wainwright, *A Coast to Coast Walk*, 1973

The power grid dates back to the late 1800's when a link was built between two generating companies to exchange power [21]. Now, our lives revolve around the use of electricity making the power grid one of societies' most critical infrastructures. What started as a small business delivering electricity to few customers with a few generating turbines and some transmission lines is now the worlds largest synchronous machine. Electricity is no longer a commodity of the few, but an essential good embedded in our everyday life. This network is a collaboration of a verity of entities that play a role in its operation, generation, transmission and distribution. The power grid's success is not a small task and it requires regulators, operators, policy makers, markets, rate design and standards to ensure a reliable supply of electricity to us, the customer, even in the face of adversity.

1.1 Motivation for Resilience

Natural disasters pose a growing threat to our society and our infrastructures. Modern life is highly dependent on infrastructures that provide essential services such as the electric, gas, transportation, water and health systems. At the same time there is interdependence between the various critical networks making their operation a multi-energy system. As we advance technology and strive to reduce emissions by electrification we are increasing the dependence on electricity for operation, relying on a secure and reliable delivery more than ever [4]; While we consider electricity an *on-demand* service, the grid is always faced

with challenges both endogenous and exogenous. At its bottom line, maintaining supply and demand is a complex problem and even more so in the *unexpected* event of a natural disaster. Power systems resilience is of growing concern with the increase in frequency and magnitude of natural events disrupting our networks and causing extended outages that have a severe impact on human life.

There is a great effort by the government and other entities, private and public, to maintain systems in operation and even more so the power system [65] [16]. Current power systems are built and operated to be able to supply demand continuously even in the event of one or two components failing i.e., being $N-1$ or $N-2$ secure. However, high impact low probability (HILP) events, such as natural disasters, can result in the sudden impairment of a larger number of components and cause outages that can take a long time to restore. For example, restoring power to all the people of Puerto Rico after the 2017 Hurricane Maria took more than 6 months. In recent years, HILP events have grown in frequency and severity, urging grid planning and operation to be more focused on making the grid more *resilient* i.e., how to better prepare, withstand and recover from extreme events. Resilience research evaluates the current state of grids, predicts climate and human behavioural patterns and assesses their impact on electricity in order to ensure future grids meet the requirements to succeed. It aims to understand threats and explore ways to prepare, withstand, recover and redesign more *resilient* grids.

1.2 Resilience Framework

There are several definitions and perspectives that build the state-of-the-art framework on resilience. According to NIAC [10], infrastructure resilience is the ability to reduce the magnitude and/or duration of disruptive events. The effectiveness of a resilient infrastructure or enterprise depends upon its ability to anticipate, absorb, adapt to, and/or rapidly recover from a potentially disruptive event. The construct presented in Fig.1.1 establishes two layers pertaining to an event, the actions taken for a specific scenario and the lessons learned that feed back into each stage. Comparably, the matrix presented in [23] depicts 4 aspects:

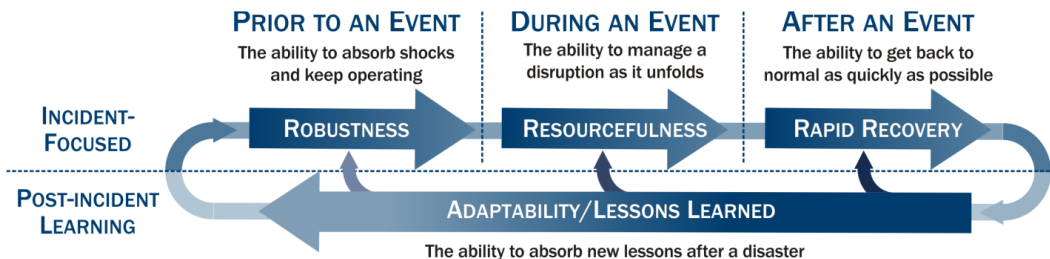


Figure 1.1: NIAC Resilience Construct [10]

technical, organizational, social and economic for each of the 4 dimensions of resilience: robustness, redundancy, resourcefulness and rapidity. For this work, we will take the following definitions:

- Robustness- the ability to absorb shocks and keep operating.
- Resourcefulness- the ability to manage a disruption as it unfolds.
- Rapid Recovery- the ability to get back to normal as quickly as possible.
- Adaptability- the ability of absorb new lessons after the disaster.

Resilience is not only focused on natural disasters, but also cyber attacks [3] [5], terrorism, communication errors [70], and cascading failures can have severe impact on power system security and operation. To have a holistic view, every piece of the puzzle must be accounted for and evaluated periodically through performance metrics and standards. Metrics are important in any evaluation process and are used to optimize performance. In the case of resilience, there are various metrics adopted by regulators and utilities mostly. At the distribution network, service based performance metrics such as loss of load expectation (LOLE), duration of outage, number of outages in a given period, and customer satisfaction are used to evaluate grid operation. At the transmission network, the metrics are rather about resource adequacy, generation capacity, flexibility and network expansion planning which

have wider implications that concern system operators and policy whereas the distribution network involves end-use costumers. While these metrics lack consistency and accuracy worldwide, in [72] metrics are developed to serve as industry guidelines along with the IEEE Std 1366(TM) with the purpose of having a benchmark for distribution system performance.

1.3 Scope of the Work and Organization

This dissertation identifies vulnerabilities in multi-energy infrastructures, evaluates interdicted operation and planning under extreme circumstances. I propose a framework that models the interactions with the natural gas network in order to holistically assess the dependencies and minimize outages during and in the aftermath of an extreme event. Optimization models are introduced to quantify power system performance, identify worst-case scenarios in a tractable and efficient manner and compare investment strategies. This research endeavor specifically answers three key questions:

1. With the current structure and resources allocated to a given grid, how can we prioritize critical load to be served during extended outages?
2. Increased penetration of gas-fired generators in our energy mix makes our power system reliant on natural gas delivery. How can we achieve a joint resilience of both infrastructures during HILP events?
3. With budget constraint investments, how do different actions from a portfolio enhance robustness against a wide range of threat magnitudes?

This thesis is organized as follows:

- Chapter 2: **Resourcefulness in Power Systems Post-Natural Disasters.** Although there are resources and protocols in place to recover and avoid extended outages during a natural disaster, the reality is that each extreme event presents its own challenges. When standard protocols fail to recover and repair quickly, the impact is

absorbed by individual customers that have to find the means on their own, not always optimally, to serve their needs. Extensive analysis is made on a case study in Puerto Rico after hurricane Maria to:

- Evaluate performance of PV-Battery systems during extended outages.
 - Design PV-Battery stand alone systems to supply critical loads.
- **Chapter 3: Joint Power-Natural Gas Infrastructure Framework for Analysis in Planning.** Power grids are not a standalone system; they interact with other infrastructures that are vulnerable to the same type of natural disasters. This chapter identifies a subset of plausible spatially-correlated components in the gas network that, when failed, produce the worst-case scenario of gas shed used for power generation. Specifically we present a
 - Tractable computational method for solving natural gas N-k interdiction problems.
 - Plausible spatially-correlated component failures that create a worst-case scenario
 - Incorporate a probabilistic model of event threats that define impact magnitudes.
 - **Chapter 4: Evaluation of Robustness Strategies Against Extreme Events.** Hardening is a regular and common practice employed to enhance existing power system assets and keep in compliance with operating standards. It is also a preventive measures against future threats. On the other hand, distributed energy resources (DERs) can provide flexibility and supply load in a decentralized manner in the event of a disruption. Both strategies aid robustness and have advantages and disadvantages. In this chapter we evaluate a portfolio of grid enhancing actions, specifically
 - Conduct a sensitivity analysis within in a portfolio of hardening and DER enhancement options.

- Optimize investments strategies to increase resilience under extreme wind speeds.
- Chapter 5: **Conclusions and Future Work** Finally, we provide a general summary of the key findings and postulate future research directions on resilience.

Chapter 2

RESOURCEFULNESS IN POWER SYSTEMS POST-NATURAL DISASTERS

Published as:

Chanaka Keerthisinghe, Mareldi Ahumada-Paras, Lilo D. Pozzo, Daniel S. Kirschen, Hugo Pontes, Wesley K. Tatum, and Marvi A. Matos., PV-Battery Systems for Critical Loads During Emergencies: A Case Study from Puerto Rico After Hurricane Maria, *IEEE Power and Energy Magazine*, vol. 17, no. 1, pp. 82-92, Jan.-Feb. 2019.

Tosado, G., Matos, M., Ahumada-Paras, M., Chapko, M., and Pozzo, L. Evaluation of Solar-Powered Battery Systems for Individuals Using Electricity-Dependent Medical Devices in Puerto Rico Following Hurricane Maria, *Disaster Medicine and Public Health Preparedness*, 1-4. 2021.

2.1 Motivation

Natural disasters often leave communities, particularly isolated rural communities, without grid connection for a long time endangering the health and life of people who rely on electrically-powered medical devices. While small systems combining photo-voltaic (PV) generation and battery energy storage could be deployed to help cope with such emergencies, very little reliable data is available on how such systems would actually be used and thus on their design requirements.

Restoration Literature Review

Utilities' approach to distribution system restoration is mainly based on predetermined priorities which tends to be sub optimal, the lack of situational awareness after the hazard significantly delays the restoration process [17]. There are several protocols that utilities and governments follow to start the restoration process. [63] summarizes the present look at practical solutions to catastrophic events that include R&D, microgrids, decentralized systems, islanding mode and enhanced communication and switching protocols. These approaches are encompassed within the pre-hazard planning of a more resilient network, nevertheless, motioned in [67] is the post-event involvement of human operators that play a key role in the operation and restoration of power systems. In [15], a code-base metric is proposed and evaluated in operational resiliency of power distributed systems using steady state and dynamic simulation tools. The key idea of the algorithm is to develop a better operating criteria focused on the critical loads.

There is ongoing research on microgrids to act as emergency sources to serve critical loads when a centralized source is unavailable. This localized strategy can help mitigate the harm done to a network and provide customers with temporary service. [71] proposes a resiliency-based methodology that uses microgrids to restore critical loads on distribution feeders after a major disaster. Stability of microgrids, limits on frequency deviation, and limits on transient voltage and current of DGs are incorporated as constraints of the critical load restoration problem. The limits on the amount of generation resources within microgrids are also considered. By introducing the concepts of restoration tree and load group, restoration of critical loads is transformed into a maximum coverage problem, which is a linear integer program (LIP). The restoration paths and actions are determined for critical loads by solving the LIP.

To properly address the critical loads first, another crucial piece of information needed is the node load prioritization. Not only the load at each node but also of the importance of the load, e.g. hospitals, fire stations, control centers, etc. A precedence and hierarchical

sequence is determined to properly dispatch repair crews.

Similarly [66] proposes a decision-making method to determine the optimal restoration strategy coordinating multiple sources to serve critical loads after blackouts. The critical load restoration problem is solved by a two-stage method with the first stage deciding the post-restoration topology and the second stage determining the set of loads to be restored and the outputs of sources. This applies to smaller outages that do not imply the whole network to be damaged. In the second stage, the problem is formulated as a mixed-integer semidefinite program. The objective is maximizing the number of loads restored, weighted by their priority. The unbalanced three-phase power flow constraint and other operational constraints are considered. An iterative algorithm is proposed to deal with integer variables and can attain the global optimum of the critical load restoration problem by solving a few semidefinite programs in most cases.

Assuming communication is available during the restoration process and not damaged along with the power assets [68] proposes a comprehensive power outage detection and service restoration framework for a distribution system with advanced metering infrastructure meters and networked microgrids. A decentralised outage detection method which obtains the total number of customers and the total amount of lost load in the outage area via local information exchanges among meters. To provide fast-response service restoration, the proposed framework incorporates the network reconfiguration and the local power support from the connected microgrids. The optimal restoration problem is formulated as a mixed-integer quadratic program that controls distributed generators and loads within a microgrid and line switches to maximise the restored critical loads.

2.2 Puerto Rico after Hurricane Maria, a Comprehensive Case Study

Hurricane Maria struck Puerto Rico on September 20, 2017 and left large parts of the island without electricity for months. As Fig. 2.1 shows, restoration in remote mountainous regions took more than 200 days.

Long-term power outages can be lethal, specially to individuals who rely on electrically-

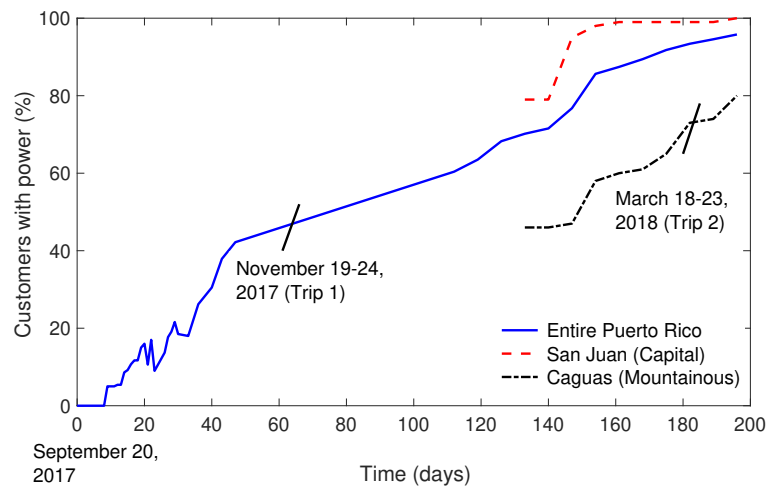


Figure 2.1: Restoration of power to customers in Puerto Rico after Hurricane Maria. Note the significant difference between the San Juan urban area and the mountainous and directly hit region of Caguas. Based on data from [45].

powered medical devices or require medicines that must be refrigerated [31]. While the initial death toll of Hurricane Maria is 64, according to [28, 29, 35], the lack of electricity raised the actual number of deaths closer to 2975. This number is calculated by comparing the total medical-related deaths during 2017 with the average numbers in the past four years. Another study [34] estimates the death toll at 4645. It is likely that remote areas were more severely affected because damaged roads not only prevented access to medical facilities but also hampered the regular delivery of medical supplies and fuel for portable generators. Small systems combining PV generation and battery storage could be deployed during such emergencies to help affected individuals cope until grid-supplied power is restored. However, very little reliable data is available on how such systems would actually be used to meet critical medical needs and thus on what their design requirements should be.

The following field project ceases the opportunity to enrich academic research on resilience with real data gathered directly from the source in the impacted community. **The main goal of this project is to collect data on how emergency systems would actually work and in parallel provide some relief donations to the most affected individuals.** This

work was conducted by researchers at the University of Washington in collaboration with community leaders in the municipality of Jayuya, a remote small town in the mountainous region of Puerto Rico.

The project entailed the following stages:

- Field trip 1: *November 2017*, conduct surveys and interviews to understand the necessities and provide immediate electricity relief to the most vulnerable households.
- Preliminary Design of PV-battery system capable of supplying medical machines.
- Field trip 2: *March 2018*, installation of PV-battery systems and logging devices.
- Field trip 3: *July 2018*, gather the data collected by these systems after several months of utilization.
- Optimization of PV-battery Systems.

Field Trip 1: Initial Survey

The main goal of the first trip was to identify, based on interviews with patients and their families, the critical medical needs that require electric power at the household level. The details on the topic guide are found in Appendix A. Then carry out a preliminary assessment of the power and energy requirements associated with these needs. The collection and analysis of data was based on households located in remote areas that were without grid-connection for more than 2 months. The critical medical conditions and associated electrical devices that were identified during these interviews are:

- Feeding machines and electrical bedding for percutaneous endoscopic gastronomy(PEG) patients
- Nebulizers or oxygen concentrators for asthma and/or chronic obstructive pulmonary disease (COPD) patients

- Continuous positive airway pressure (CPAP) machines for sleep apnea patients
- Refrigeration for medicines, such as insulin for diabetic patients, and food for patients with special dietary requirements. Note that a higher than average proportion of Puerto Rico's population suffers from diabetes [29].

Dialysis and treatments for other acute medical needs were not included in this assessment because they are usually not carried out at home and critical patients are frequently evacuated before or after emergencies.

Interviews also revealed some of the ways in which individuals coped with the lack of electricity. PEG patients used gravity feeding instead of powered peristaltic pumps, which resulted in substantially faster feeding. Many of the diabetic patients kept their insulin cool either by using water and ice or moving their refrigerators to nearby businesses that had emergency generators. However, some stopped taking insulin out of fear that it had degraded. Since the local clinic was without power until a backup generator arrived, they lost medicines requiring refrigeration as well as all vaccines. Other loads common to all households were perceived as important but less critical: refrigeration for regular food, fans, lighting, television and washing machines (particularly important in households with bedridden patients). Cooking appliances do not appear on this list because most households in this part of Puerto Rico use gas for this purpose.

Basic information about critical loads were complemented by reading manufacturer's labels and by asking families how often each appliance was used and for how long. During the interviews, we explicitly asked the families to state the power ratings and the time-of-use of their critical loads summarized in Table 2.1. There was no electricity after the hurricane, so we did not have a way to measure actual load profiles. The measured power was obtained during the third field trip.

Table 2.1: The maximum and average measured power, time-of-use and duration of critical electrical loads.

Device name	Duration	Use per day	Average power	Maximum power
PEG feeding machine	30 minutes	4 times	less than 10 W	120 W
Electrical bed	30 seconds	10 times	18 W	53-65 W
Inflatable mattress	8-24 h	-	less than 10 W	10 W
Nebulizers	5-25 minutes	2-4 times	23-52 W	23-66 W
Oxygen concentrators	Up to 24 h	-	350 W	428 W
CPAP	9 h	10 pm - 7 am	34 W	47 W
Refrigerator	8-24 h	-	136-352 W	140-392 W
Refrigerator (small)	8-24 h	-	20 W	97 W
Television	2-4 h	3-9 pm	28-292 W	31-392 W

Preliminary Design

The initial scope and preliminary data served to design solutions to aid individuals reliant on electricity. Taking advantage of the sunny weather in Puerto Rico (not during a hurricane) we developed standalone PV-battery systems for emergency response designed with 3 different sizes adjusting to the information gathered in Table 2.1. Due to budget, time restrictions, and inaccurate load profiles generated on the basis of the limited information the systems were limited in capacity, nevertheless, we anticipated that the systems would be able to meet at least some of the critical loads of individual households either fully or in tandem use with diesel generators. However, although commonly used in emergencies, diesel generators were perceived as having the following drawbacks:

- Our interviews revealed that some asthma and COPD patients had worsened because of the exhaust gases (such as carbon monoxide) or the aerosolized soot particles produced by the diesel engines [42, 59].

- Due to noise, generators cannot be used at night to power the CPAP machines of sleep apnea patients.
- Reliable access to a supply of diesel fuel during an emergency can be difficult or impossible, particularly in remote areas.
- Using a generator can cost up to \$10 per day. Over an extended period of time, this can be excessive for low income households
- Emergency diesel generators are often not designed for continuous use. Individuals would have to use them for periods of 2-6 hours. For example, some households ran diesel generators up to eight hours per day to keep medicines cool. There were also many instances where generators had broken down because of overuse.
- Maintaining a generators (i.e. changing the oil) is challenging for some users because it requires time, knowledge and money.

Depicted in Fig 2.2 is one system that consists of a 1 kW inverter, maximum power point tracking (MPPT), solar charge controller, display monitor, data loggers, lead-acid batteries (inside the box), and data loggers to record the electrical load profiles, PV output, battery *state-of-charge* (SoC) and temperature.

Field Trip 2: Deployment

The goal of the second field trip was to install 17 standalone PV-battery systems of 4 different types and power ratings. A summary of the installed systems is given in Table 2.2. System Types A (Fig. 2.2), B and D were designed at University of Washington, while system Type C was a commercial system.

Since there were more households with critical medical needs than available systems, the households considered for installations were chosen according to the following criteria: first condition was that the inhabitants must rely on electrically-powered medical devices or have

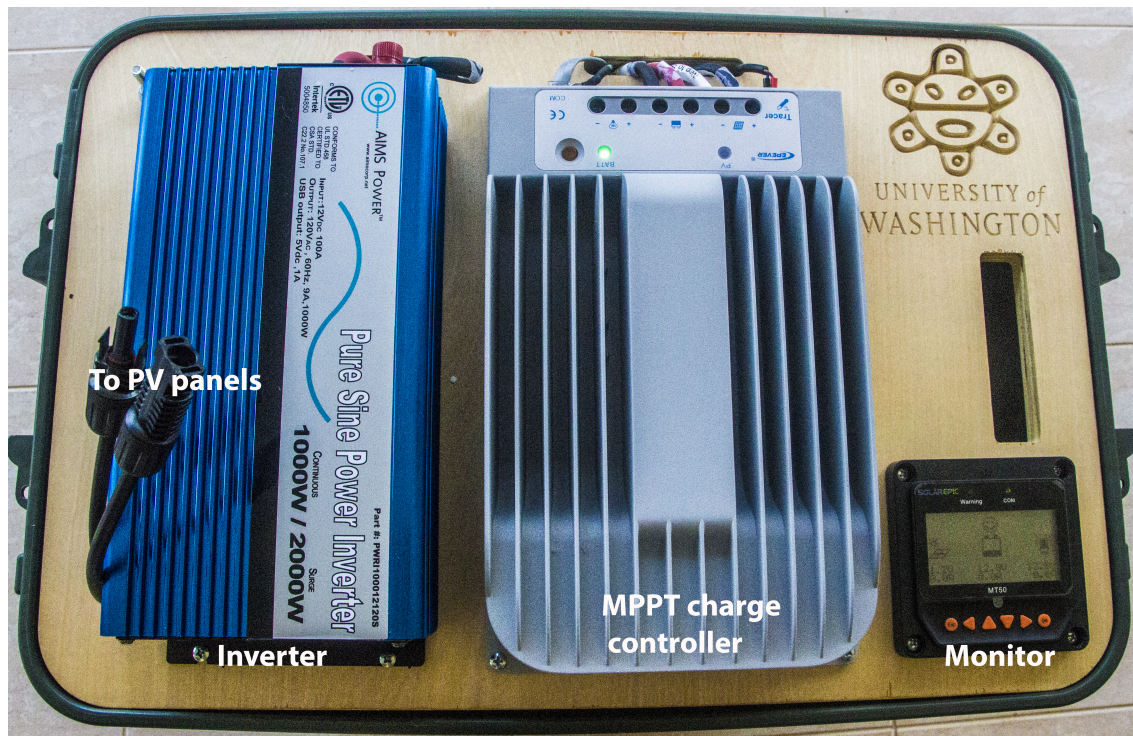


Figure 2.2: Top view of a PV-battery system designed at the University of Washington. Note that the batteries, data logger and majority of the cables are inside the box.

medical-related refrigeration requirements. Second condition was the lack of resources to buy or obtain their own source of electricity. Third was their geographical location. Higher priority was given to the people living in the mountains with limited accessibility.

We advised users to not discharge their batteries below recommended safety limits e.i. a minimum *depth-of-discharge* (DoD), in order to optimize the lifetime of the battery. Other instructions include: safety precautions, details about the system configuration and required information to expand their system.

Field Trip 3 : Analysis of the Standalone PV-Battery Systems

One the third trip we obtained data collected by the data loggers in the installed PV-battery systems. Satisfaction surveys were also administered to gauge the user experience

Table 2.2: Summary of the systems installed.

	PV size (W)	Battery	MPPT	Inverter (kW)	Number of installations
Type A	260	160 Ah (lead-acid)	yes	1	6
Type B	100-200	80-100 Ah (lead-acid)	no	1	6
Type C	400	1.1 kWh (lithium-ion)	yes	1.1	5
Type D	100	100 Ah (lead-acid)	no	DC system	4

and perception of solar energy as a form of emergency energy supply. This quantitative and qualitative data is analyzed to properly size systems in future emergency response projects. Data included electrical load profiles, PV output, battery SoC, and temperature.

Fig.2.3 illustrates load profiles of the days with highest energy consumption. Important findings are as follows: Households 1-6 used most of their devices during the day when there is sun in order to maximize their battery lifetime. However, they ended up using the battery a lot during the day to compensate for varying solar irradiance so therefore, expedited the battery degradation. Note that the PV systems given to Households 1-6 are only 260 W. The largest load profile from Fig.2.3 is used to construct the critical load percentages in Table 2.3 of 6 different households that vary in family size, location, medical conditions and have diesel generator accessibility. The important finding here is that for Households 1 and 2 the critical load is 17.2% and 15.4%, respectively, of their household load before the hurricane. Unfortunately, we were not able to obtain the loads before the Hurricane Maria for some households.

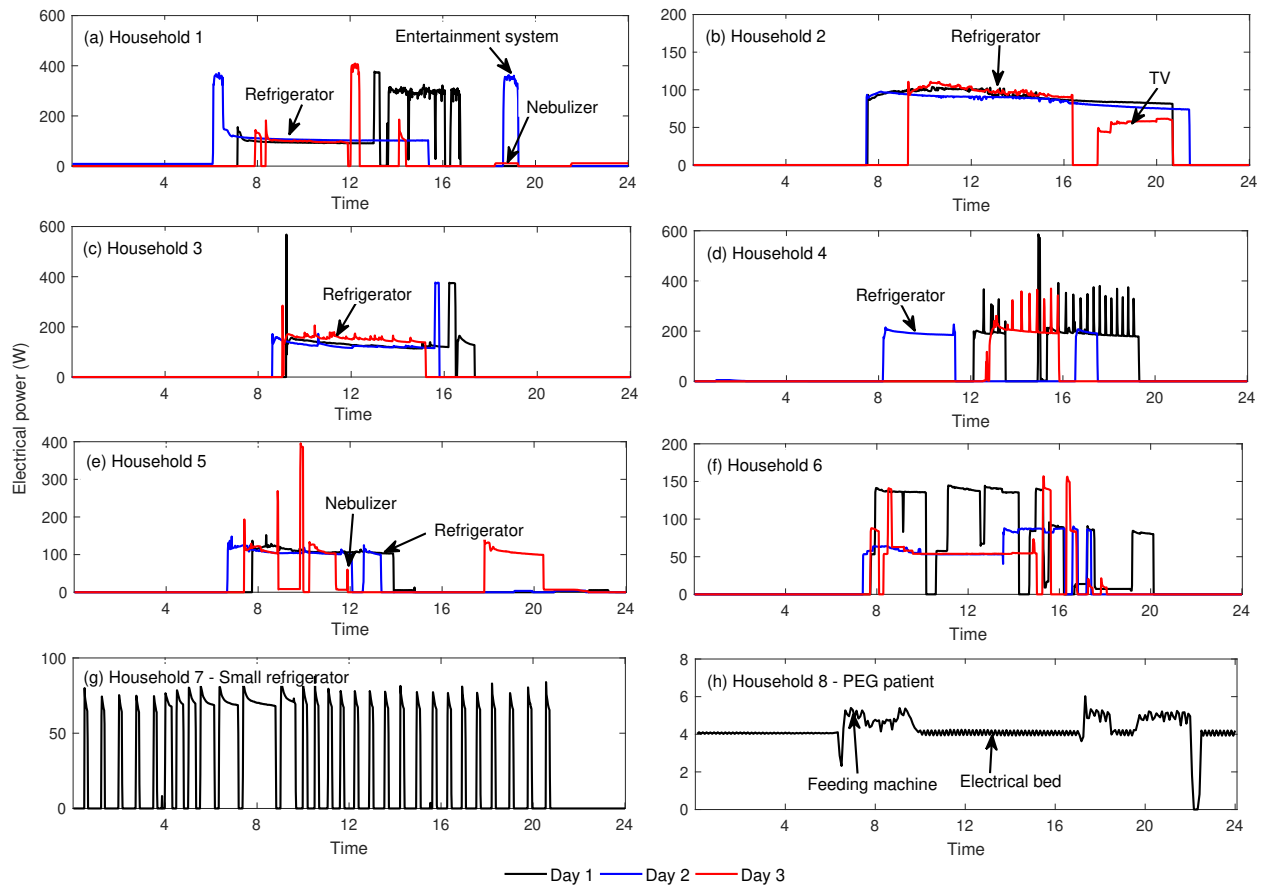


Figure 2.3: Electrical load profiles of eight different households over one to three days.

The total daily energy consumption and PV generation over 47 days for 6 households is shown in Fig.2.4. Key findings include the energy use pattern for Household 6 is similar to the PV generation pattern, which shows the users managed to consume the PV generation on the same day. This energy consumption pattern contributed to keeping their battery in good condition. Other important finding is that Households 4 and 5 stopped using the systems after they regained grid power within one month after our installation while other users continued to use the systems throughout the whole period.

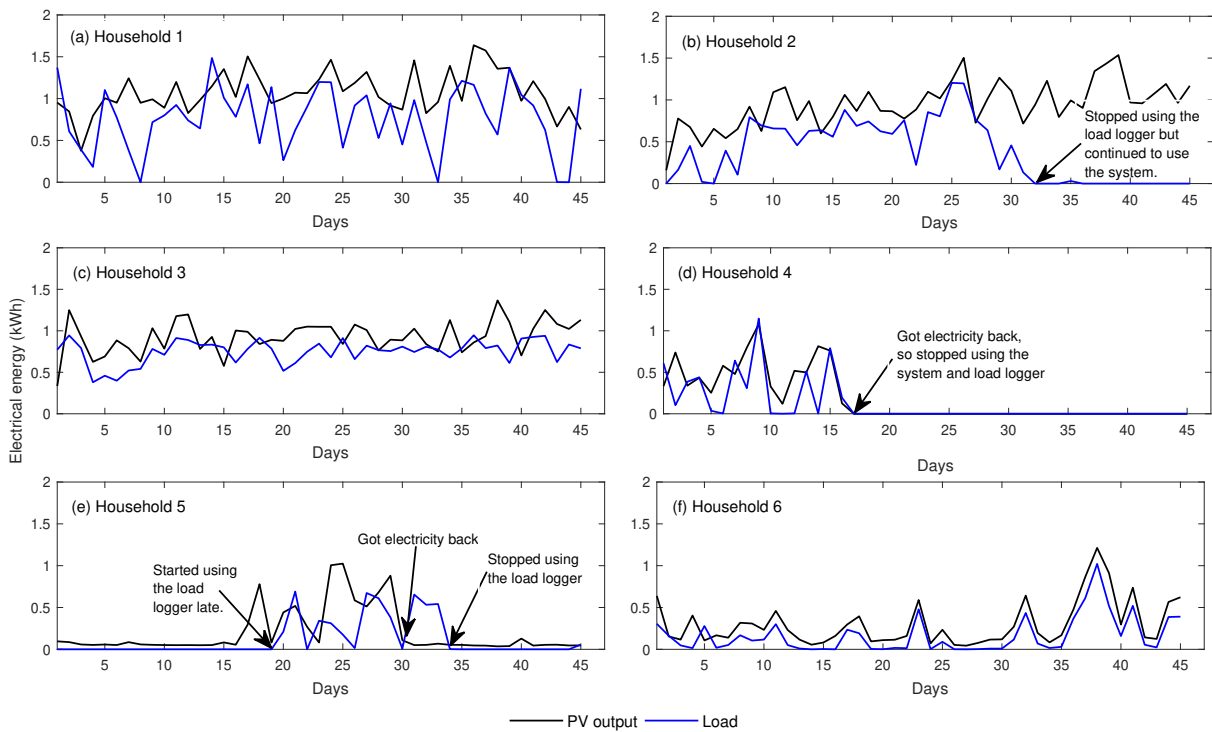


Figure 2.4: Generation and consumption for 8 households during a 3 day period

Battery degradation

In this section we investigate the battery degradation issues associated with lead-acid batteries of our PV-battery systems. Our systems are not equipped with battery management systems (BMSs) to limit the DoD, however, we instructed the user to operate the battery within safety limits. As depicted in Fig. 2.5(a), Households 6 and 5 were cautious about the DoD while Households 1, 2 and 3 were not. We noticed that the lead-acid battery of Household 6 was in perfect condition while Household 2 users said that their battery was not performing in the way that it originally used to. This may be a sign of decreased capacity due to degradation after repeated cycling at more than 50% DoD.

The temperature of the batteries also affects the battery lifetime. Even in the high tropical temperatures of Puerto Rico, the battery temperatures were generally found to be

Table 2.3: Energy consumption details of the six households.

Household:	Critical load (kWh/day)	Load before hurricane (kWh/day)	Critical load percentage (%)	Cost of generator fuel (\$/day)
1	1.5	8.67	17.2	10
2	1.2	7.77	15.4	7
3	1.2	-	-	10
4	1.1	-	-	-
5	0.7	7.5	9.2	-
6	1	-	-	-

within expected limits 20–25°C, with the exception of one household where the temperature increased up to 30°C, as depicted in Fig. 2.5(b). Note that the temperature of Household 5 is slightly higher compared to the other households that are in the mountains.

2.3 Optimal PV-Battery Design

Given these insights, we propose an efficiently sized resilience-oriented PV-battery systems for disaster response using critical load profiles collected from the load and PV-battery data loggers in our installed systems. Specifically, the system capacity is based on a continuous operation over a year considering battery degradation, PV projections, and load variations. Finlay, the benefits of PV-storage systems are also compared to those of using a diesel generator.

The reason we only consider standalone systems is because the focus here is on disaster recovery. For the sake of completion we briefly describe important design consideration about grid-connected systems in Puerto Rico. There is no need for the battery to be charged

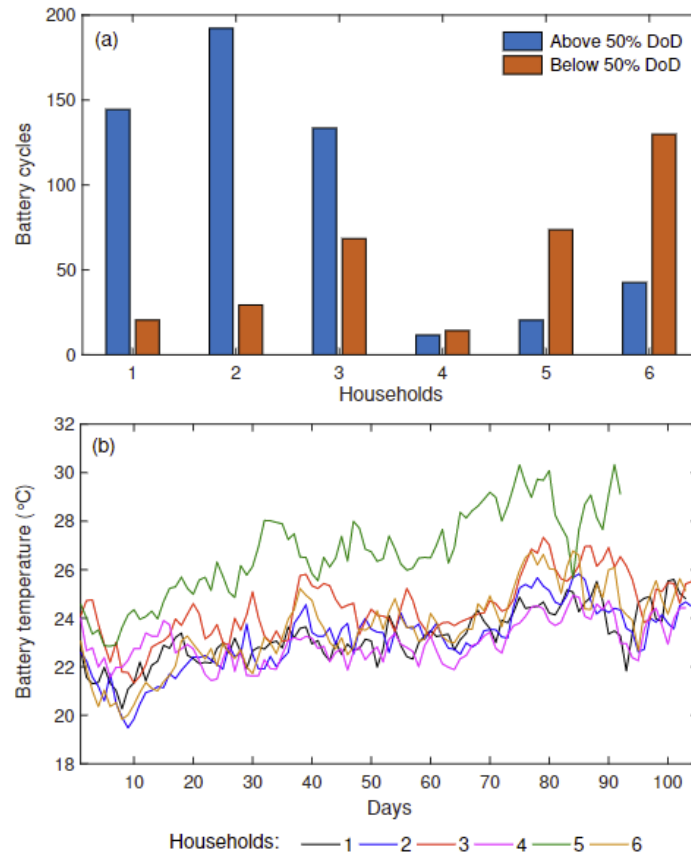


Figure 2.5: Battery degradation studies: (a) number of battery cycles over 50% DoD and 50% or less DoD for six households; and (b) average daily battery temperature for six households over 105 days.

by the electrical grid because electricity prices in Puerto Rico are constant. Note that if the electricity price is not constant (i.e. time-varying), we would need to use an energy management system to seize the full potential of the PV-battery system. If this were the case the underlying problem would be a stochastic optimization problem because of the uncertainty associated with the PV output, electrical demand and electricity prices. Secondly, the PV and battery size are designed for continuous operation in islanded mode. This saves the need for an expensive bi-directional inverter. Also the size of the battery only depends on the ability to power critical loads during an emergency because there is no need to maximize the

self-consumption of solar power since Puerto Rico has net metering.

Problem Formulation

Variables:

s_k^b - Battery SoC

x_k^b - Battery charge and discharge rates

s_k^{pv} - PV output

s_k^d - Electrical demand

p - System size

P - Number of Systems to compare

R - Continuous Operation Time (COT)

Efficiencies:

$\mu^{b,d}$ - Battery discharging

$\mu^{b,c}$ - Battery charging

μ^i - Inverter

Algorithm 1 used to size the resilience-oriented PV-battery systems proceeds as follows:

1. First load hourly electrical load and PV output profiles over a year. Also define the efficiencies for battery charging and discharging and inverter (Lines 1-2).
2. Define the duration of the required COT, R . For 1 year, $R=8760$ (Line 3).
3. $\forall pinP$, All portfolio of systems included in the optimization. Note that our aim is to obtain the required battery capacity given the PV system size and COT. k denotes a particular time-step over the year (Lines 4-5).
4. Let: $\mathbf{s}^b = [s_k^b \dots s_{k+R}^b]$, $\mathbf{s}^d = [s_k^d \dots s_{k+R}^d]$,
 $\mathbf{s}^{pv} = [s_k^{pv} \dots s_{k+R}^{pv}]$ and $\mathbf{x}^b = [x_k^b \dots x_{k+R}^b]$. Calculate battery discharge rate that is

required to provide resilient power over the given duration and the maximum possible battery charge rate from solar:

$$\mathbf{x}^b = \begin{cases} \mathbf{s}^{\text{pv}} - (1/\mu^i)\mathbf{s}^{\text{d}}, & \text{if } \mathbf{s}^{\text{pv}} - (1/\mu^i)\mathbf{s}^{\text{d}} \geq 0 \\ \mathbf{s}^{\text{pv}} - (1/\mu^{\text{b,d}})(1/\mu^i)\mathbf{s}^{\text{d}}, & \text{otherwise} \end{cases}, \quad (2.1)$$

Note that the above battery decisions are positive for battery charging and negative for discharging. The battery only discharges to supply the load and when the battery charge rate is zero or more then the load is met by the solar system. The battery charge rate from Eq. (2.1) is the maximum possible battery charge rate used in the optimization, however, the actual charge rate may vary depending on the size of the battery (Lines 6-7).

5. Optimize the battery SoC needed to provide power over the given duration.

$$\min F = c^b \mathbf{s}^b, \quad (2.2)$$

where c^b is the cost of a battery per kWh and F is the objective function. The battery SoC evolves according to:

$$s_{k+1}^b = s_k^b + (\mu_k^{\text{b,c}})x_k^{\text{b+}} - x_k^{\text{b-}}. \quad (2.3)$$

6. The maximum value from each optimization is the minimum required battery capacity to provide resilient power over the given duration (Line 10)
7. Calculate the number of battery cycles for the given battery capacity (Line 11) and finally, calculate the total cost of the system using the PV system size, battery size and degradation costs (Line 12).

Algorithm 1 : Algorithm for sizing resilience-oriented PV-battery systems

Input: PV output and electrical load data over a year

Input: Battery and inverter efficiencies

- 1: Define the resilience duration (i.e. 1 year)
 - 2: **for** $p = 1, \dots, P$ **do**
 - 3: **for** $k = 1, \dots, R = 8760$ **do**
 - 4: Calculate battery discharge rates that are required to provide resilient power over the given duration.
 - 5: Calculate the maximum possible battery charge rate.
 - 6: Optimize the battery SoC needed to provide power over the given duration.
 - 7: The maximum battery SoC from the optimization is the minimum battery capacity required for the given COT.
 - 8: Calculate the battery cycles corresponding to the optimum battery capacity.
 - 9: Obtain the total cost of the system given the PV system size, battery size and the battery degradation costs over year.
-

2.4 Simulation Results

We consider four different scenarios as follows:

- Scenario A is for Household 1's critical load profiles in Fig. 2.3(a). These load profiles include a refrigerator, which was managed efficiently, Nebulizer and an entertainment system. This household was without electricity for over 10 months and the inhabitants found above loads to be critical.
- Scenario B is for a household with a PEG patient and has a small refrigerator. The critical load profile is a combination of Fig. 2.3(g) and (h).
- Scenario C is for a household with a sleep apnea patient. The critical loads are the CPAP machine, refrigerator and a TV. The critical load profile for this scenario is created using the data in Table 2.1.

- Scenario D has the largest critical load, which consist of a oxygen concentrator that runs 24h, refrigerator and TV.

PV output data for the optimizations are from the National Renewable Energy Laboratories' (NREL) PVwatts calculator [44]. We assume that a lead-acid battery can last 200 cycles when the DoD is above 50% and increases to 500 cycles when the DoD is below 50% [8].

A summary of the simulation results for the four scenarios over a year is given in Table 2.5 and more details about sizing procedure of Scenario A is shown in Fig. 2.6. Increasing the the PV system size decreases the minimum battery capacity required to provide continuous power to the critical loads, as depicted in Fig. 2.6(a). Note that we are only interested in finding out the minimum battery capacity required to provide resilient power to the critical loads so extra PV generation is curtailed instead of increasing the battery size to store the excess PV generation. The battery cost per kWh (192 per lead-acid and 800 per lithium-ion) is much higher compared to the PV cost per W (\$0.75-1.5) so the cost of the system decreases as the battery size decreases in Fig 2.6(b).

The lowest cost systems for Scenarios A, B and C are using lead-acid batteries because the cost of smaller-scale lithium-ion batteries (i.e. 100 Ah) are still much higher compared to the larger-scale batteries (i.e. 12 kWh Tesla Powerwall). In particular, lead-acid batteries with 100% DoD is the cheapest because the combination of PV and battery systems are effectively sized to minimize the number of battery cycles. Moreover in some scenarios, such as Household 1, inhabitants used their critical loads mostly during day so the requirement for battery power is minimum. Another reason is that we only consider battery cycle cost over year because these systems are for emergencies only. Note that battery degradation due to the battery use during the day was a main concern with our installed systems, therefore, in order to overcome that the proposed systems have higher PV system sizes. This means on sunny days the users have extra solar energy during the day to be used for other loads otherwise the solar charge controller will curtail the excess power.

On the other hand, Scenario D requires a larger system so it is economically beneficial

to install this as a grid-connected system and operate it for non-emergencies as well. The battery system will be using lithium-ion as it is cheaper for larger-scale systems and saves space. The cost of the Scenario D system is based on a 0.75\$ per W for PV and 195\$ per kWh battery (i.e. Tesla Powerwall). This scenario is shown for the sake of completion, a detailed economic analysis of grid-connected systems is not the focus of this paper.

In summary, our proposed systems' sizes for Scenarios A, B and C can be used as a guideline for dispatching PV-battery systems for future emergencies. Regarding the battery technology, it is important to note that the lithium-ion batteries are the most convenient as they are smaller in size and less heavy compared to lead-acid batteries. This would make it easier for the user to move their systems around the house as well as the installers with transportation. In future, the cost of lithium-ion batteries will continue to decrease and will hopefully replace the lead-acid batteries as the cost-optimal technology.

A comparison of cost of a generator and PV-battery system is given in Fig. 2.7 for a long power outage. The capital cost of the generator is low compared to the PV-battery system, however, the on going costs due to fuel, oil change and depreciation is very high. On the other hand, PV-battery systems have a slightly higher capital cost but the ongoing costs due to battery degradation and depreciation is much lower compared to the generator. Our conclusion is that any place that is likely to experience more than 40 days (cumulative) of power outages (even over multiple events) would benefit from a PV system. Longer usage loads (CPAP, air mattress, oxygen concentrator etc) may inevitably need PV systems since they need long term use that is difficult to achieve with small diesel/gas generators.

2.5 Summary

Our simulations showed that a system with 500 W_p PV and 270 Ah lead-acid battery is enough to power a small critical medical device (i.e. nebulizer, CPAP or feeding machines), refrigerator and small television while maximizing the battery lifetime. This project fully analyzed research findings and data collected during the three Hurricane Maria disaster recovery field trips to Puerto Rico by the researchers at the University of Washington. The

resilience-oriented PV-battery systems proposed in this paper using critical load profiles collected in Puerto Rico will be helpful for governments and emergency service organizations with their humanitarian work after natural disasters. The systems were optimally sized according to the critical load identified. The benefits of using standalone PV-battery systems over a diesel generator to supply critical loads have been evaluated for different time scales.

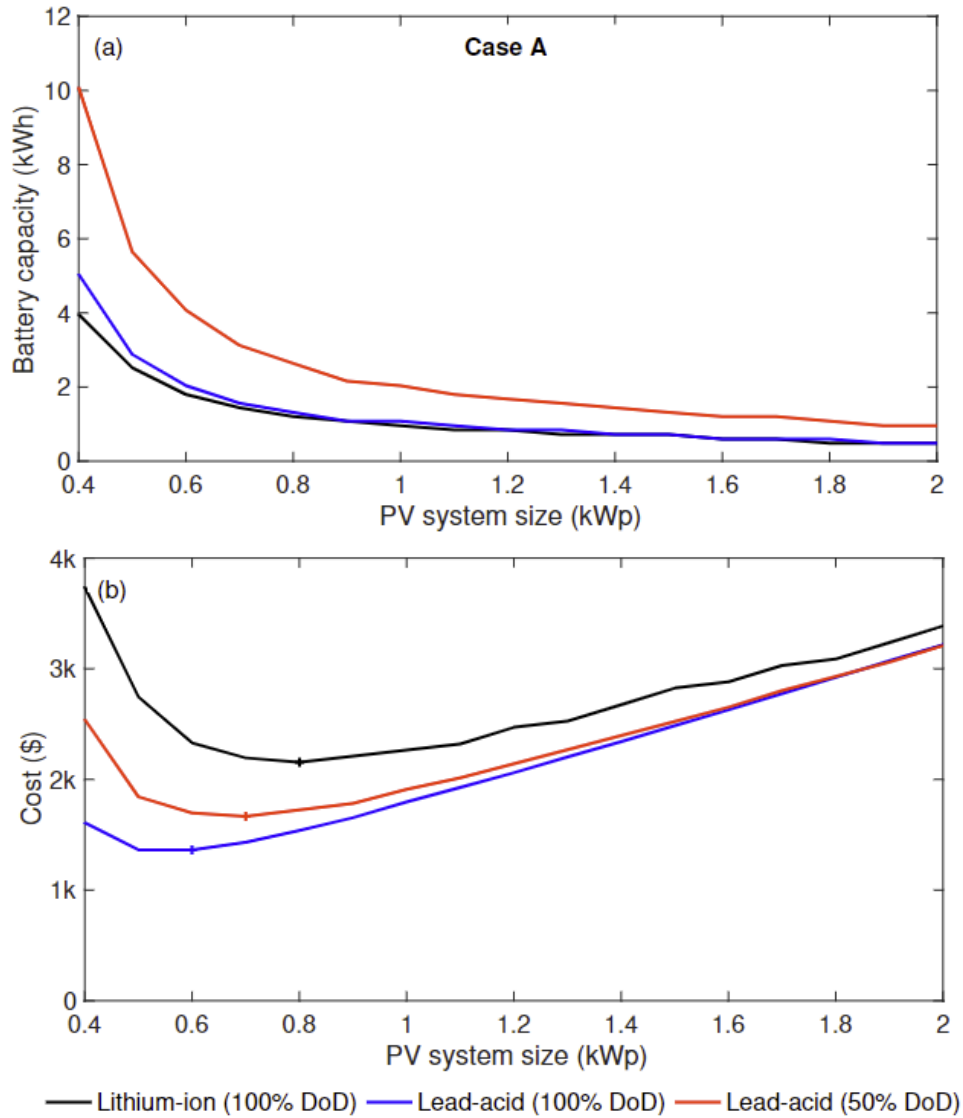


Figure 2.6: Scenario A: (a) the minimum battery capacity required to power critical loads over a year against the PV system size; and (b) total PV and battery cost against the PV system size.

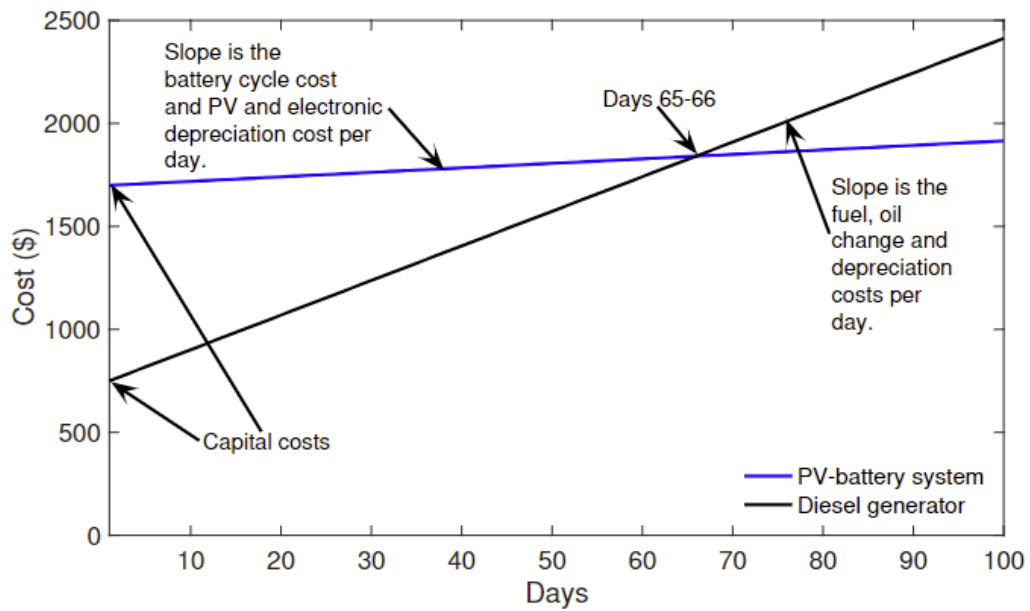


Figure 2.7: Cost of using a diesel generator and PV-battery system after a disaster.

Table 2.4: Comparison of various PV-battery system designs. The cost only consists of the PV and batteries and r is the number of battery replacements.

Battery type and DoD	Battery size (Ah) @12V	PV size (Wp)	Total PV (kWh)	Total load (kWh)	Battery cycles (1 year)	Battery cycles (3 years)	Battery cycles (5 years)	Battery cycles (10 years)	Cost (US\$) (1 year)	Cost (US\$) (3 years)	Cost (US\$) (5 years)	Cost (US\$) (10 years)
Case A - Refrigerator, nebulizer and TV												
Li-ion (100% DoD)	100	800	1291	484	78	235	392	783	2150 $r=0$	2150 $r=0$	2150 $r=0$	2150 $r=0$
Lead-acid (100% DoD)	170	600	968		63	188	313	626	1291 $r=0$	1291 $r=0$	1682 $r=1$	2464 $r=3$
Lead-acid (50% DoD)	260	700	1130		36	107	178	356	1648 $r=0$	1648 $r=0$	1648 $r=0$	1648 $r=0$
Case B - PEG patient and small refrigerator												
Li-ion (100% DoD)	60	300	484	197	166	497	828	1655	1020 $r=0$	1020 $r=0$	1020 $r=0$	1020 $r=0$
Lead-acid (100% DoD)	120	200	323		92	275	458	916	576 $r=0$	852 $r=1$	1128 $r=2$	1680 $r=4$
Lead-acid (50% DoD)	120	300	484		88	263	438	876	726 $r=0$	726 $r=0$	726 $r=0$	1002 $r=1$
Case C - CPAP, refrigerator and small TV												
Li-ion (100% DoD)	120	700	1130	459	245	735	1225	2450	2190 $r=0$	2190 $r=0$	2190 $r=0$	2190 $r=0$
Lead-acid (100% DoD)	270	500	807		117	351	585	1170	1371 $r=0$	1992 $r=1$	2613 $r=2$	4476 $r=5$
Lead-acid (50% DoD)	290	700	1130		108	324	540	1080	1717 $r=0$	1717 $r=0$	2384 $r=1$	3051 $r=2$
Case D - Oxygen concentrator, refrigerator and TV												
Li-ion (100% DoD)	950	4900	7907	3594	219	656	1093	2185	5900 $r=0$	5900 $r=0$	5900 $r=0$	5900 $r=0$
Lead-acid (100% DoD)	2070	3800	6132		108	324	540	1080	-	-	-	-
Lead-acid (50% DoD)	1980	5500	8875		110	331	552	1103	-	-	-	-

Chapter 3

JOINT POWER-NATURAL GAS INFRASTRUCTURE FRAMEWORK FOR ANALYSIS IN PLANNING

Published as:

Mareldi Ahumada-Paras, Kaarthik Sundar, Russell Bent, and Anatoly Zlotnik. N-k interdiction modeling for natural gas networks. *Electric Power Systems Research*, 190:106725, 2021.

Mareldi Ahumada-Paras, Rodrigo Moreno, Daniel Kirschen. N-k Analysis of Natural Gas Systems Under Natural Disasters and the Impact on Power Generation, *IEEE Power & Energy Society General Meeting (PESGM)*, 2022.

We use bi-level formulation to optimize operational decisions in the first level against worst-case gas shed scenarios found in the second level. This model is computationally efficient to determine worst-case scenarios to advise on expansion planning models.

3.1 Motivation

Natural disasters can be devastating, not only during the actual event but also in its aftermath where various infrastructure's lack of functionality impairs our lifestyles. These events jeopardize every component in their path, be it from the power, water, gas or transportation network. There is a spatial correlation between failures in these systems. Such a correlation affects how we analyze and assess resilience. For example, dangerous situations could be mitigated or avoided if operators of the power and natural gas systems plan for possible interactions and inform each other about events in their network during a disturbance. A recent event highlighting the importance of power-gas dependencies under natural disasters

was the outage in Texas, USA in February of 2021, where the sudden drop in temperature, froze the gas pipeline system and decreased the generating power capacity causing a widespread outage.

When talking about resilience, it is essential to consider not only the electricity grid but also the other infrastructures that either depend on the grid or affect the operation of the grid. The interdependence between the electricity and natural gas systems is of particular interest because over the last decade, U.S. natural gas deliveries to electric power consumers more than doubled, with the power sector’s share of the total natural gas demand growing from 22.3% to 35.5% [30]. This sharp increase in interdependence is driven by the growing number of gas-fired power plants, which is itself the result of two main factors. First, low natural gas prices have made gas generators competitive in power markets. Second, because of the increasing penetration of variable energy resources such as wind and solar, backup generation must be available to compensate for their variability. Gas-fired power plants are able to respond rapidly and on-demand. Consequently, these gas-fired power plants account for more than half of the total gas off-takes in some market regions in the United States [30]. However, their intermittent operation affects the amount of natural gas drawn from delivery points and hence the overall operation of gas networks.

Our investigation is motivated by the increased reliance of many power systems on natural gas-fired generation, which is used to meet increasing production requirements, replace retiring coal and nuclear plants, and provide controllable resources to compensate for the variability from renewable sources like wind and solar [38]. Gas-fired generators now supply a significant fraction of base electric power production in many countries, which creates a fundamental reliance of power grids on gas pipelines for just-in-time fuel delivery. As a result, it has become increasingly likely that unplanned component outages or other contingencies in a natural gas pipeline could cause correlated (large k) electricity generator outages [37,50]. We develop an approach to support the identification of sets of $N-k$ scenarios in gas pipeline networks that induce large failures in a dependent power system. We also demonstrate the method on models of the Belgian and New England natural gas pipeline networks, as well

as the gaslib-582 test instance.

Although electricity transmission systems are typically very robust, the impacts that arise when they are disrupted motivate methods for analyzing outage risk. For example, N - k interdiction models were developed to characterize disruptions by identifying the sets of k power system components whose failure results in “worst case” outages. While such models have advanced considerably, they generally neglect how failures outside the power system can cause large-scale outages. Specifically, failures in natural gas pipeline networks that provide fuel for gas-fired generators can affect the function of the power grid. In this study, we extend N - k interdiction modeling to gas pipeline networks. We use recently developed convex relaxations for natural gas flow equations to yield tractable formulations for identifying sets of k components whose failure can cause curtailment of natural gas delivery. We then present a novel cutting-plane algorithm to solve these problems. Finally, we use test instances to analyze the performance of the approach in conjunction with simulations of outage effects on electrical power grids.

In power system operations and planning, N - k contingency analysis is used to assess system reliability and resilience. In these analyses, k components are turned “off” in a computational model of the electrical grid and system-wide effects of this removal are modeled through a computer simulation. These simulations use optimal power flow (OPF)-like optimization models, such as maximal load delivery [19], to estimate outages caused by a contingency.

Contingency analysis is often combined with N - k interdiction modeling to identify sets of k components whose simultaneous failure leads to the worst outcome (typically outages) during a contingency analysis. While solving an interdiction problem itself is challenging, the state-of-the-art has improved considerably over the last several decades and (at least heuristic) solutions are regularly reported on problems with large N and k (see [12, 25, 33, 46, 51, 52, 56] and references therein).

One of the weaknesses of N - k analysis, in particular for large k , is that it is often implausible for the identified k components to fail simultaneously, i.e., they are geographically

separated by a large distances. This has led to the development of new models and methods for identifying sets of k components whose concurrent failure is more likely [56], or that constrain the possibilities of the interdiction plan [57]. In this article, in order to further address this limitation in traditional power system interdiction modeling, we develop an approach for identifying failures in a power system that are caused by exogenous failures, which, in this case, arise in natural gas pipeline networks that deliver fuel to gas-fired generators.

3.2 Gas Network Framework

In comparison with power systems literature, there are relatively few studies that apply contingency analysis and interdiction modeling to natural gas pipeline systems. In one study, the authors suggest gas pipeline networks as natural candidates for interdiction modeling [69], but do not discuss the complexities associated with modeling natural gas systems in interdiction problems. As a result, many subsequent papers have relied on enumeration methods, used simplified models that neglect the physics of natural gas flows, or are restricted to small problems. For example, one study focused on developing a vulnerability assessment approach in which all combinations of failures up to size k are enumerated, and then performs a max-flow calculation (that does not account for natural gas flow physics) on a 33-node system [55].

The effect that interdicting a gas pipeline network has on a power system that relies heavily on natural gas for generation is another area that has received limited attention. The most relevant study on the behavior of a power system after a natural gas pipeline failure is reference [49]. In this study, the authors develop a model that enumerates all single failures ($N-1$) in a gas pipeline and then use the results to identify generator outages and security constraint violations in the power system. They do not model the response of the power system, nor does the paper seek to identify the “worst” k -outage for a gas network. References [22, 40, 64] are the most closely related works to this paper. These studies focus on developing tri-level models for the design or hardening of electric power and natural gas delivery systems such that the lost demand after a worst case k -outage scenario is minimized.

To preserve tractability, linear approximations of gas flows are used and empirical results are limited to systems with no more than 40 nodes in the gas pipeline network.

In this study, we focus on the details of natural gas physical flow modeling in interdiction and, for the first time, *relaxations* of the gas flow are used, which in contrast to approximations are able to provide guarantees on solution quality as well as to scale to a case study with 582 nodes (in a bi-level model).

In summary, the contributions are:

- A comprehensive $N-k$ interdiction model for natural gas systems based on recently developed convex relaxations for gas pipeline networks.
- A tractable computational method for solving natural gas $N-k$ interdiction problems.
- A detailed case study that examines how an $N-k$ interdiction on a gas pipeline network impacts an associated electric power system by estimating the potential loss of generation on gas-fired generators on that system.
- A framework to delimit $N-k$ analysis under the impact of a natural disaster. We consider a deterministic $N-k$ worst case scenario of natural gas system with spatially-correlated failures. This is done by delimiting the components at risk of failure within a defined impacted area \mathcal{A} as a result of a specific event such as an earthquake, hurricane or wildfire.
- After interdicting power and natural gas networks, we compare the damaged power network against a baseline operation.
- Probabilistic approach [47] where there is an analysis of event probability and component fragility curves.

3.3 Problem Formulation

The goal of the $N-k$ interdiction problem for natural gas pipeline networks is to identify k components in the gas network that, when damaged, have the greatest impact on the transportation capacity of the system. For these systems, we measure impact by computing the minimum amount of gas that the system is unable to provide to delivery points, relative to the baseline (unaffected) flow allocation. A subset of these delivery points correspond to power plants that use the natural gas to generate electricity.

Formally, the $N-k$ problem is stated as follows: given a natural gas pipeline network with nodes \mathcal{N} , pipelines, \mathcal{P} , and compressors \mathcal{C} , an $N-k$ interdiction problem identifies k components in $\mathcal{P} \cup \mathcal{C}$ whose loss maximizes the minimum amount of un-served gas loads at delivery points. Gas is injected into or withdrawn from the system from a subset of nodes (receipt and delivery points, \mathcal{R} and \mathcal{D} , respectively) in the network. The max-min structure makes the $N-k$ interdiction problem a bi-level optimization problem. These problems are often modeled as Stackelberg games with an attacker and a defender [14], where the attacker's and defender's actions are sequential and the attacker has a perfect model of how the defender will respond to an attack. Such problems are NP-Hard [56] because of the inherent combinatorial nature of the problem. Furthermore, the number of possible $N-k$ contingencies, even for small values of k , makes complete enumeration intractable. This makes such models difficult to scale to large systems, which is a prerequisite to apply the desired interdiction modeling in practice.

The following notation is used for indexing sets, decision variables, and parameters in the optimization formulation:

Sets:

\mathcal{A} - Set of natural disaster impacted elements

\mathcal{X} - $N-k$ contingency scenario set $\in \mathcal{A}$

Power Network Sets:

\mathcal{B}, \mathcal{E} - sets of buses and edges

\mathcal{G}, \mathcal{L} - sets of generators and loads

$\mathcal{G}(i), \mathcal{L}(i)$ - sets of generators and loads at bus i

$\mathcal{G}(x)$ - sets of damaged generators in scenario $x \in \mathcal{X}$

$\mathcal{E}_p(i)$ - subset of lines connected to bus i and oriented *from* i

$\mathcal{E}_p^r(i)$ - subset of lines connected to bus i and oriented *to* i

Gas Network Sets:

$\mathcal{N}, \mathcal{C}, \mathcal{P}$ - sets of nodes, compressors and pipes

\mathcal{R}, \mathcal{D} - sets of receipt and delivery points

$\mathcal{R}(i), \mathcal{D}(i)$ - sets of receipt and delivery points at node i

$\mathcal{C}(x), \mathcal{P}(x)$ - sets of damaged compressors and pipes in scenario $x \in \mathcal{X}$

$\mathcal{E}(i)$ - subset of pipes and compressors connected to node i and oriented *from* i

$\mathcal{E}^r(i)$ - subset of pipes and compressors connected to node i and oriented *to* i

Decision variables:

π_i - square of pressure at node i (Pa^2)

f_e - mass flow rate across $e \in \mathcal{C} \cup \mathcal{P}$ (kg s^{-1})

s_i - total gas produced at receipt points in $\mathcal{R}(i)$ (kg s^{-1})

λ_i - unserved gas-factor for each node $i \in \mathcal{N}$

γ_e - auxiliary variable for each pipe $e \in \mathcal{P}$

y_e - binary flow direction variable for each $e \in \mathcal{C} \cup \mathcal{P}$

x_e - binary interdiction variable for each $e \in \mathcal{C} \cup \mathcal{P}$

$\mathbf{V}_i = v_i \angle \theta_i$ - AC voltage at bus i

$\mathbf{S}_i^g = p_i^g + \mathbf{i}q_i^g$ - AC power generated at bus i

$\mathbf{S}_{ij} = p_{ij} + \mathbf{i}q_{ij}$ - AC power flow across $e \in \mathcal{E}$

σ_i - cost coefficients $i \in \mathcal{G}$

\mathbf{x} - vector of interdiction variables x_e

Parameters:

\mathbf{d}_i - total gas delivered at delivery points in $\mathcal{D}(i)$ (kg s^{-1})

\mathbf{w}_e - resistance of the pipe $e \in \mathcal{P}$

\mathbf{a} - speed of sound in the gas (m s^{-1})

β_e - friction factor of the pipe $e \in \mathcal{P}$

ℓ_e, D_e - length, diameter of the pipe $e \in \mathcal{P}$ (m,m)

$(\underline{\pi}_i, \bar{\pi}_i)$ - min and max limits for π_i (Pa^2)

$(\underline{\alpha}_e, \bar{\alpha}_e)$ - min and max compression limits for $e \in \mathcal{C}$

f_e - max flow rate for $e \in \mathcal{C} \cup \mathcal{P}$ (kg s^{-1}) $\mathbf{S}_i^d = p_i^d + \mathbf{i}q_i^d$ - AC power demand at bus i in $\mathcal{L}(i)$ (kg s^{-1})

$\mathbf{Y}_{ij} = g_{ij} + \mathbf{i}b_{ij}$ - admittance of line $e \in \mathcal{E}$

t_{ij} - thermal limit of line $e \in \mathcal{E}$

$(\underline{v}_i, \bar{v}_i)$ - min and max limits for voltage magnitude at bus i

$(\underline{p}_e, \bar{p}_e)$ - min and max active power for $e \in \mathcal{G}$

$(\underline{q}_e, \bar{q}_e)$ - min and max reactive power for $e \in \mathcal{G}$

θ_{ij}^Δ - max phase angle difference across line $e \in \mathcal{E}$

3.3.1 Steady State Gas Flow Equations

Before presenting the formulation, we review the physics that govern steady flow of natural gas through pipelines. The physics of flow across a pipeline, $e = (i, j)$, are described by a set of partial differential equations (PDEs) that have dimensions in both time and space [60].

In steady-state, the PDEs reduce to equations of the form

$$\pi_i - \pi_j = \mathbf{w}_e f_e |f_e|, \quad (3.1)$$

where the phenomenological expression on the right hand side quantifies the dissipation of kinetic energy caused by turbulent flow through the pipe. The parameter \mathbf{w}_e is called a resistance factor, and is given by

$$\mathbf{w}_e = \frac{4\beta_e \ell_e \mathbf{a}^2}{\pi^2 D_e^5}. \quad (3.2)$$

For a detailed derivation of the parameters in this equation, interested readers are referred to [58]. To compensate for the dissipation of energy along the direction of flow, a gas pipeline utilizes compressors to boost flow and pressure throughout the system. We model these components as short pipes with zero resistance values, which create a jump in pressure while preserving flow in the direction of the compressor's orientation. When the gas flows through the compressor in the opposite direction of its orientation, the compressor is assumed to not offer any pressure boost.

3.3.2 Power Model

For completeness the power flow model described is a simplified representation with $\zeta(\mathbf{x})$ as the objective cost function for all generators obtained from [20]. There is no intent to contribute to the state-of-the-art power flow models.

$$\zeta(\mathbf{x}) = \min \sum_{i \in \mathcal{G}} \sigma_i \operatorname{Re}(\mathbf{S}_i^g), \quad (3.3a)$$

$$\mathbf{S}_{ij} = \mathbf{Y}_{ij}^* \mathbf{V}_i \mathbf{V}_i^* - \mathbf{Y}_{ij}^* \mathbf{V}_j \mathbf{V}_j^* \quad \forall e \in \mathcal{E}_p \cup \mathcal{E}_p^r, \quad (3.3b)$$

$$\sum_{e \in \mathcal{E}_p} \mathbf{S}_{ij} - \sum_{e \in \mathcal{E}_p^r} \mathbf{S}_{ji} = \mathbf{S}_i^g - (1 - \sigma_i) \mathbf{S}_i^d \quad \forall i \in \mathcal{B}, \quad (3.3c)$$

$$\underline{v}_i \leq |V_i| \leq \overline{v}_i \quad \forall i \in \mathcal{B}, \quad (3.3d)$$

$$\underline{p}_e \leq \operatorname{Re}(\mathbf{S}_i^g) \leq \overline{p}_e \quad \forall e \in \mathcal{G}, \quad (3.3e)$$

$$\underline{q}_e \leq \operatorname{Im}(\mathbf{S}_i^g) \leq \overline{q}_e \quad \forall e \in \mathcal{G}, \quad (3.3f)$$

$$|\mathbf{S}_{ij}| \leq \mathbf{t}_{ij} \quad \forall (i, j) = e \in \mathcal{E}_p \cup \mathcal{E}_p^r, \quad (3.3g)$$

$$-\boldsymbol{\theta}_{ij}^\Delta \leq V_i V_j^* \leq \boldsymbol{\theta}_{ij}^\Delta, \forall (i, j) = e \in \mathcal{E}_p, \quad (3.3h)$$

where Eq. (3.3a) is the problem objective. Eqs. (3.3b) and (3.3c) represent the power flow and power flow balance, respectively. Eqs. (3.3d) – (3.3h) are the operating limits for voltage, active power, reactive power, thermal and angle difference.

3.3.3 N - k interdiction problem for Gas Network

The N - k interdiction problem is formulated as follows:

$$\max_{\mathbf{x} \in \mathcal{X}} \eta(\mathbf{x}), \quad (3.4)$$

where $\mathcal{X} = \{\mathbf{x} : \sum_{e \in \mathcal{C} \cup \mathcal{P}} x_e = k\}$ and $\eta(\mathbf{x})$ is the total amount of gas unserved at all delivery points in scenario \mathbf{x} . The elements of \mathcal{X} correspond to N - k contingency scenarios and are implicitly defined by the variables in \mathbf{x} that take value 1. The core sub-problem for the N - k problem is the Minimal Gas Shedding (MGS) problem that defines the value of $\eta(\mathbf{x})$ as

$$\eta(\mathbf{x}) = \min \sum_{i \in \mathcal{N}} \lambda_i \mathbf{d}_i, \quad (3.5a)$$

$$\pi_i - \pi_j = \mathbf{w}_e |f_e| f_e \quad \forall (i, j) = e \in \mathcal{P} : x_e = 0, \quad (3.5b)$$

$$\pi_i - \pi_j = 0, \text{ if } f_e \leq 0, \forall (i, j) = e \in \mathcal{C} : x_e = 0, \quad (3.5c)$$

$$\underline{\alpha}_e^2 \pi_i \leq \pi_j \leq \bar{\alpha}_e^2 \pi_i, \text{ if } f_e \geq 0, \forall (i, j) = e \in \mathcal{C} : x_e = 0 \quad (3.5d)$$

$$\sum_{e \in \mathcal{E}(i)} f_e - \sum_{e \in \mathcal{E}^r(i)} f_e = s_i - (1 - \lambda_i) \mathbf{d}_i \quad \forall i \in \mathcal{N}, \quad (3.5e)$$

$$\underline{\pi}_i \leq \pi_i \leq \bar{\pi}_i \quad \forall i \in \mathcal{N}, \quad (3.5f)$$

$$-\mathbf{f}_e \leq f_e \leq \mathbf{f}_e \quad \forall e \in \mathcal{C} \cup \mathcal{P}. \quad (3.5g)$$

The formulation for MGS, as stated in Eq. (3.5), is a non-linear disjunctive formulation. Eq. (3.5b) denotes the steady-state gas flow physics for each pipe that has not been damaged by the N - k scenario, and Eq. (3.5e) enforces a mass flow balance condition at each node in the system. The Eqs. (3.5c) and (3.5d) deactivate pressure boosting and enforce boosting limits of a compressor with flow directed against and along the orientation of the compressor, respectively. Finally, Eqs. (3.5f) and (3.5g) enforce pressure and flow rate limits on each node and pipe in the network, respectively. The above formulation is a bi-level optimization problem where the outer maximization problem is given by Eq. (3.4) and inner minimization problem is given by Eq. (3.5). Appendix B details the a Mixed-Integer Non-Linear Programming (MINLP) reformulation and a Mixed-Integer Second-Order Cone

Programming (MISOCP) relaxation of the MGS using binary flow direction variables y_e for each compressor and pipe in the network.

3.3.4 Joint Power-Gas Network

In order to examine the effects $N-k$ gas contingencies have on power systems, we use models which connect the gas networks to the power systems [9] as depicted in Fig. 3.1. In particular, gas-fired generators are attached to nodes in the natural gas networks. These generators withdraw gas from the natural gas pipeline network, and unserved gas load implies that gas-fired power plants receive insufficient gas and operate with reduced capacity. The power withdrawn at compressor stations in the gas network is neglected. The loss in gas-fired generation capacity is computed using heat rate curves that convert mass flow (kg/s) into available MW capacity. In particular, the burn-rate, i.e., the gas withdrawal d_i from the gas pipeline network at node $i \in \mathcal{N}$, is converted into power production profiles p_g for a generator $g \in \mathcal{G}$ in the power network using a quadratic heat rate curve

$$p_g(\mathbf{d}_i) = \beta_0 + \beta_1 \mathbf{d}_i + \beta_2 \mathbf{d}_i^2. \quad (3.6)$$

In Eq. (3.6), the units of p_g is MW, and that of β_0, β_1 , and β_2 are MW, MW kg^{-1} , and $\text{MW s}^2 \text{kg}^{-2}$

3.3.5 Threat Model

This framework, displayed in Fig. 3.1, represents a simplified holistic view of the network interactions under the impact of a natural disaster. We define a threat with an impact area, \mathcal{A} , where components from both networks inside the area are susceptible to failure. This area represents a plausible set of attacked components connected spatially. Depending on the strength and type of the event, the area can expand to those components adjacent to the initial impact.

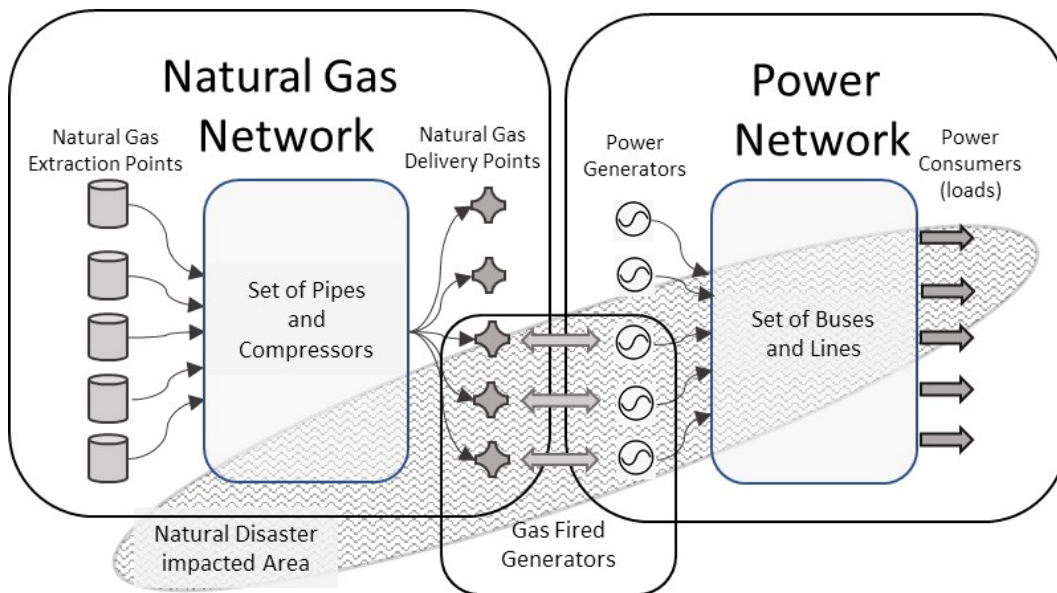


Figure 3.1: Power and natural gas network structures and the area impacted by a single natural disaster event.

Initially, to evaluate in a toy model setting, we have 3 levels of intensity $\mathcal{A} = 25, 50$ and 100 % of the total network components. Each event characterization can include likelihood of path, severity and component fragility curves under different stresses such as wind speed, flooding, earthquakes or extreme weather.

A risk-based probabilistic approach in [47] mentions the need to evaluate the operational and planning aspects through resilience metrics and modifying fragility curves according to each unique situation. In [1] any component is subject to failure regardless of topology or physical location since the scope was delimited to simultaneous failures, we identify a realistic scenario by correlating the components and restricting the impact. Fig. 3.2 depicts an example of how a deterministic $N-k$ interdiction analysis can be restricted depending on epicenter and impact radius of earthquakes.

Lastly, an earthquake model is used for proof of concept. It is built from historic data on earthquakes in Chile and simulations including location, depth, magnitude, peak ground

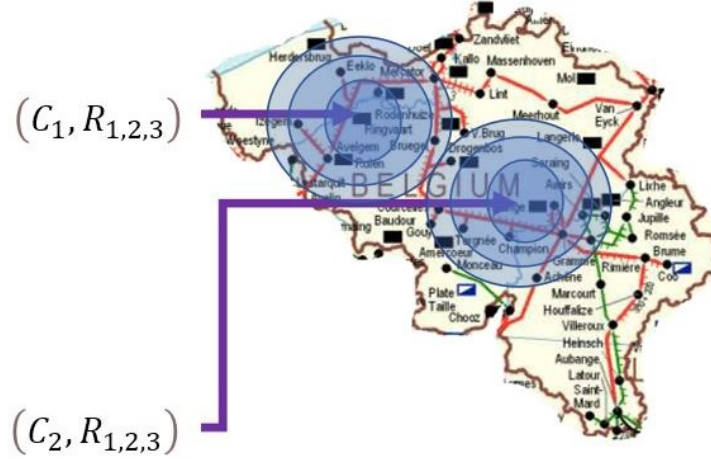


Figure 3.2: Area defined by an epicenter C and a radius R that represents a given earthquake strength and location.

acceleration.

$$\log_{10}[PGA(r, h, M)] = -1.55 + 0.26M + 0.01h - 0.01R - (1.52 - 0.10M) \cdot \log_{10}R \quad (3.7)$$

where, M is magnitude in Gutenberg-Richter scale and the hypocenter is a function of coordinates.

3.4 Proposed Method

In this section, we present a generic cutting-plane algorithm that works directly with the bi-level structure of the $N-k$ problem. A number of techniques have been proposed to convert such a bi-level max-min problem into a single mixed-integer program (see [2, 43]). Given the recent success of algorithms that directly exploit the bi-level structure in problems concerning electric transmission systems [56, 57], we adopt them here. The algorithm is generic and is applicable to the MINLP and the MISOCP relaxations as long as they are solved to global optimality. In this article, we restrict our attention to using the algorithm on the MISOCP

relaxation of the MGS problem, because it can be solved to global optimality with off-the-shelf commercial or open-source solvers. The algorithm generates cutting planes using solutions of the inner problem, and adds them sequentially to the outer problem.

The algorithm constructs a sequence of piecewise linear functions that bounds from above the total curtailment of scheduled gas delivery given by solutions to the inner problem or its MISOCP relaxation. For any $N-k$ scenario, $\hat{\mathbf{x}}$, $\eta(\hat{\mathbf{x}})$ denotes the minimum unserved gas for that scenario as given by (3.5) or its MISOCP relaxation. Then, the algorithm computes coefficients $\delta_e(\hat{\mathbf{x}})$ for each $e \in \mathcal{C} \cup \mathcal{P}$ such that

$$\eta(\mathbf{x}) \leq \eta(\hat{\mathbf{x}}) + \sum_{e \in \mathcal{C} \cup \mathcal{P}} \delta_e(\hat{\mathbf{x}}) \cdot x_e \quad \forall \mathbf{x} \in \mathcal{X}. \quad (3.8)$$

The linear cut in (3.8) is general and there are many choices for the cut coefficients $\delta_e(\hat{\mathbf{x}})$. The key challenge is to choose *tight* values for each coefficient that do not remove the optimal $N-k$ scenario. For the $N-k$ problem in gas pipeline networks, the coefficients $\delta_e(\hat{\mathbf{x}})$ are computed using a combination of the inner problem solution for the $N-k$ scenario $\hat{\mathbf{x}}$ and the physics that governs the steady state flow of gas through the network. Using the inequality in (3.8), the bi-level problem is equivalently written as

$$(\mathcal{F}) \quad \max \eta(\mathbf{x}) \quad \text{subject to:} \quad (3.9a)$$

$$\eta(\mathbf{x}) \leq \eta(\hat{\mathbf{x}}) + \sum_{e \in \mathcal{C} \cup \mathcal{P}} \delta_e(\hat{\mathbf{x}}) \cdot x_e \quad \forall \hat{\mathbf{x}} \in \mathcal{X}, \quad (3.9b)$$

and the algorithm generates a subset of the cuts listed in Eq. (3.9b). The pseudo-code for the cutting-plane algorithm is shown in Algorithm 2, where the procedure for computing the cut coefficients (line 3.8-8) is detailed in a forthcoming paragraph.

We now present a technique for computing the coefficients $\delta_e(\hat{\mathbf{x}})$ in Eq. (3.9b) given an $N-k$ scenario $\hat{\mathbf{x}}$ and the solution of the MISOCP relaxation of the inner problem (MGS). We first present the mathematical expression of the coefficients and then provide an intuitive justification. The MISOCP relaxation of the inner problem, for a given $N-k$ scenario $\hat{\mathbf{x}}$ (let \hat{s} denote the corresponding scenario) gives the value of the mass flow rate, $f_e(\hat{\mathbf{x}})$, for every $e \in \mathcal{C} \setminus \mathcal{C}(\hat{s})$ and $e \in \mathcal{P} \setminus \mathcal{P}(\hat{s})$. For the sake of clarity, the dependence of mass flow rates on

Algorithm 2 Cutting-plane algorithm: pseudo-code

Input: optimality tolerance, $\varepsilon > 0$

Output: $\mathbf{x}^* \in \mathcal{X}$, an ε -optimal solution

- 1: initial problem: \mathcal{F} without constraint (3.9b)
 - 2: $\eta^* \leftarrow -\infty$ ▷ lower bound on the optimal obj. value
 - 3: $\bar{\eta} \leftarrow +\infty$ ▷ upper bound on the optimal obj. value
 - 4: $\hat{\mathbf{x}} \leftarrow$ any initial N - k scenario
 - 5: solve MISOCP relaxation of MGS using $\hat{\mathbf{x}}$ and let $\eta(\hat{\mathbf{x}})$ be the objective value
 - 6: **if** $\eta(\hat{\mathbf{x}}) > \eta^*$ **then** $\eta^* \leftarrow \eta(\hat{\mathbf{x}})$ and $\mathbf{x}^* \leftarrow \hat{\mathbf{x}}$
 - 7: compute $\delta_e(\hat{\mathbf{x}})$ for every $e \in \mathcal{C} \cup \mathcal{P}$ satisfying (3.8)
 - 8: add $\eta(\mathbf{x}) \leq \eta(\hat{\mathbf{x}}) + \sum_{e \in \mathcal{C} \cup \mathcal{P}} \delta_e(\hat{\mathbf{x}}) \cdot x_e$ to \mathcal{F} and resolve
 - 9: update $\hat{\mathbf{x}}$, and set $\bar{\eta}$ using solution from Step 8
 - 10: **if** $\bar{\eta} - \eta^* \leq \varepsilon \eta^*$ **then** (\mathbf{x}^*, η^*) is the ε -optimal solution, stop
 - 11: return to step: 5
-

scenario $\hat{\mathbf{x}}$ is shown explicitly. The pipes and compressors that constitute the scenario \hat{s} or equivalently, $\hat{\mathbf{x}}$, are damaged and hence do not have any gas flowing through them. Given these flow rates, the coefficients are computed by:

$$\delta_e(\hat{\mathbf{x}}) = \begin{cases} |f_e(\hat{\mathbf{x}})| & \text{if, } e \notin \hat{s} \\ 0 & \text{otherwise.} \end{cases} \quad (3.10)$$

Intuitively, setting the coefficients according to Eq. (3.10) imply that when a pipe or compressor (say e) is removed from a gas network, at most $|f_e|$ will go unserved. This statement is quantitatively true, except in the case of the Braess paradox in natural gas networks [6]. The Braess paradox occurs when adding one or more edges to a transport network can reduce overall throughput under certain conditions. Because a Braess-like condition would be a sub-optimal direction for minimizing the objective function, the paradox does not arise, and thus the coefficient values specified in (3.10) lead to a valid constraint at each iteration. The algorithm 2 ultimately converges to an ε -optimal solution to the MISOCP relaxation of the $N-k$ problem.

In addition, the following modifications to algorithm 2 are made to include Natural disaster delimitation and computing OPF.

Algorithm 3 Modified Pseudo-code

Given: An event with an impact area \mathcal{A}

Input: optimality tolerance, $\varepsilon > 0$

Output: $\mathbf{x}^* \in \mathcal{X} \subset \mathcal{A}$, an ε -optimal solution

- 1: Compute Algorithm 2 : \mathcal{F}
 - 2: Adjust \bar{p}_e and $\bar{q}_e \forall e \in \mathcal{G}$ ▷ Generator capacity
 - 3: solve OPF with $\zeta(\hat{\mathbf{x}})$ as the objective value
 - 4: stop
-

Algorithm 3 reads as as follows: given an impacted area, \mathcal{A} that contains components from a power network (buses \mathcal{B} , lines \mathcal{L} , generators G) and a natural gas network (nodes

\mathcal{N} , pipelines \mathcal{P} , and compressors \mathcal{C}), compute an N - k interdiction problem that identifies k components in $\mathcal{N} \cup \mathcal{P} \cup \mathcal{C}$ that maximize the unserved gas. After calculating the unserved gas at delivery points of the natural gas network, a power flow of the damaged power system will be compared to the baseline operation.

Scope delimitation are as follows: natural disaster modeling does not represent the cascading failures of one specific event type, but represents the potential impact of multiple failures in both systems simultaneously. This assumption will be maintained, since the study of cascading failures uses transient models of both systems in a timescale that is not relevant to a larger time-horizon in the aftermath of an extreme event. Regardless of the unfolding of a specific event, e.g. hurricane path, an earthquake epicenter, or a wind/snow storm or extreme temperatures, all components included in the final impacted \mathcal{A} will be subject to failure.

3.5 Results

In this first results section, we present case studies on three networks: (i) the Belgian gas network [24] with a total of 42 pipes and compressors that can be interdicted, (ii) the New-England (NE) natural gas network [9] with 192 pipes and compressors that can be interdicted, and (iii) the gaslib-582 test network [53] with a total of 629 pipes and compressors that can be interdicted. The Belgian and the NE case studies are simplified network models of actual gas pipeline systems in Belgium and the New England region, respectively. The k values for each run of the N - k algorithm is varied from 1 to a value where 100% of the gas load in the system is left unserved by the resulting ε -optimal, N - k contingency. For the gaslib-582 test case, due to the excessive computation time, we restrict the runs to a k value where $> 95\%$ of the gas load is left unserved. The value of ε , the optimality tolerance in Algorithm 2, is set to 0.01% for every run of the algorithm and all the formulations and algorithms were implemented in the Julia programming language using optimization layer JuMP v0.18.6 [27]

and GasModels v0.3.5¹. Finally Gurobi v8.0 was used to solve the MISOCP relaxation of the MGS (the inner problem) for the cutting-plane generation algorithm on a machine with an Intel(R) Core(TM) i7-8700 CPU 3.20GHz. We use models which connect the Belgian and the NE gas networks to the IEEE 14-bus and 36-bus test systems, respectively [9].

3.5.1 Performance of the Cutting-Plane Algorithm

First, we present computational results that corroborate the effectiveness of the cutting-plane algorithm in computing ε -optimal ($\varepsilon = 0.01\%$) N - k attacks for the three test systems. Tables 3.1 – 3.3 show the computation time, the percentage of scheduled gas delivery that was curtailed, and the number of iterations taken by the cutting-plane algorithm to compute the ε -optimal N - k attack for the Belgian, NE, and gaslib-582 cases, respectively for different values of k .

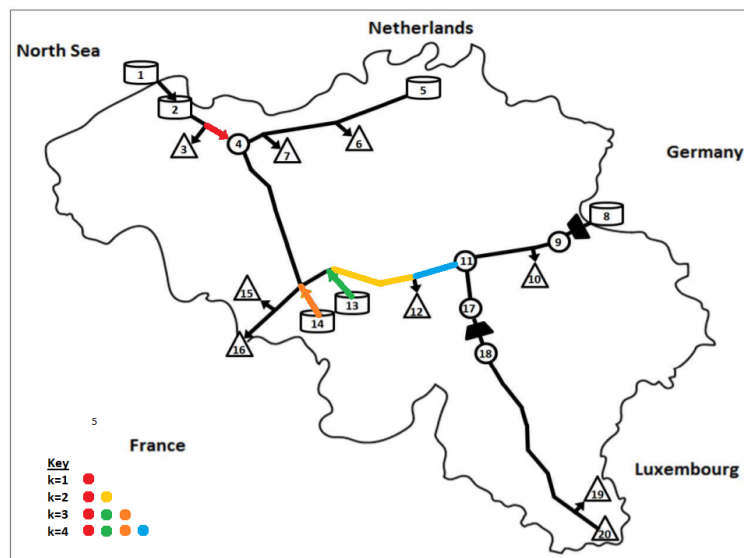


Figure 3.3: Belgian Network with interdicted components in worst case scenarios for $k = 1, 2, 3, 4$

¹<https://github.com/lanl-ansi/GasModels.jl>

Fig. 3.3 shows the components in the Belgian network that, when interdicted, produce the worst case scenarios for values of k ranging from 1 through 4. Note that the worst k -outage scenarios are a collection of nested sets. It is observed from the tables that for small values of k , $k = 2$, the Belgian, NE, and gaslib-582 cases result in 50%, 40%, and 72%, respectively, of curtailed gas load with respect to the total baseline load levels without outages. This shows the value of developing an algorithm to compute a worst case $N-k$ attack even for small values of k . Though the runs for $k \geq 5$ might not seem realistic, i.e., more than 4 components in the gas network failing simultaneously is highly unlikely, these results are shown in order to illustrate the computational limits of our algorithm and can be used as a surrogate to show the fact that our algorithm would scale to large instances with small values of k . Furthermore, from the iterations column in all the three tables it is clear that the cutting-plane algorithm is effective in computing the ε -optimal solution using only a few iterations. We remark that the computation time of the cutting-plane algorithm is in general proportional to the number of iterations of the algorithm and not related to the value of k . This trend is seen in the results for the NE test case in Table 3.2, though computation time does not always increase with k as the problem is highly nonlinear and solution time depends on initialization. Finally, from Table 3.3, it is clear that despite the low number of iterations of the algorithm even in the larger gaslib-582 case, the computation time per iteration increases because of larger MISOCP problem size for the inner computation in the larger test case.

3.5.2 Gas-fired Generation Capacity Loss in the Power Grid

This section presents results that illustrate the impact that $N-k$ gas pipeline contingencies have on electricity transmission networks. We use loss of generation capacity on all the gas-fired generation plants as a measure to quantify this impact. This study is performed only on the Belgian and the NE test cases which were connected to the IEEE 14-bus and 36-bus test systems, respectively. The Belgian-IEEE 14 system is commonly used in the literature for gas-electric system case studies, and the NE-36 bus system is another larger test case.

Table 3.1: Belgian gas network results

k	Iterations	Unserved gas (%)	Time (s)
1	4	29.4	0.163
2	4	50.4	0.109
3	4	75.1	0.104
4	7	88.9	0.147
5	6	95.1	0.125
6	8	98.0	0.247
7	9	99.3	0.267
8	13	100.0	0.348

Tables 3.4 and 3.5 show lost generation capacity (absolute value (MW) and as a percentage of total power produced by gas-fired generation in the baseline scenario) when the worst case $N-k$ occurs on the gas side. Capacity loss is computed by converting unserved gas to power consumption (MW) using quadratic heat rate curves for gas-fired power plants (Eq. (3.6)).

This article presents the first systematic algorithm to compute worst-case $N-k$ contingencies on natural gas pipeline networks by modeling relaxations of steady-state gas flow physics. The computational effectiveness of the algorithm, its scalability, and the potential use of such a tool to estimate the impact of a worst-case $N-k$ contingency on the bulk-electric system were shown through extensive computational experiments on case studies involving several widely available test networks.

3.5.3 Joint Power and Natural Gas

In Table 3.6, we compare the load shed % in the gas system and its coupled loss of generating capacity in (MW) for three different area strengths. When the whole network is available for interdiction at $\mathcal{A} = 100\%$, we obtained the same results published previously in [1].

Table 3.7 demonstrates that while having similar gas shed values, the loss of power

Table 3.2: New England gas network results

k	Iterations	Unserved gas (%)	Time (s)
1	2	24.3	3.619
2	4	39.1	5.742
3	12	47.3	15.633
4	19	56.1	27.088
5	15	64.3	23.107
6	17	71.3	23.373
7	16	77.7	21.722
8	12	83.6	14.312
9	9	89.9	10.242
10	7	94.3	9.986
11	7	97.7	8.393
12	9	99.6	9.117
13	14	99.7	15.115
14	24	99.8	34.880
15	28	99.9	73.066
16	32	100.0	716.366

Table 3.3: gaslib-582 results

k	Iterations	Unserved gas (%)	Time (s)
1	4	43.3	162.917
2	4	72.0	350.705
3	7	84.6	315.970
4	11	91.6	411.532
5	16	95.9	287.466

Table 3.4: Generation capacity loss for the Belgian-IEEE 14 network. During normal operation the power produced from all the gas-fired power plants is 39.67 MW

k	Loss of capacity (MW)	Loss of capacity (%)
1	13.52	34.09
2	23.22	58.52
3	31.25	78.78
4	37.15	93.63
5	39.34	99.16
6	39.34	99.16

Table 3.5: Generation capacity loss for the New England-IEEE 36 network. During normal operation the power produced from all the gas-fired power plants is 513.21 MW

k	Loss of capacity (MW)	Loss of capacity (%)
1	129.63	25.26
2	138.39	26.97
3	252.03	49.11
4	319.03	62.16
5	372.38	72.56
6	379.37	73.92
7	405.72	79.06
8	427.22	83.24
9	462.14	90.05
10	485.21	94.54
11	501.92	97.80
12	511.57	99.68

Table 3.6: Gas Shed and Lost Power Capacity per Damaged Area Size For Belgian-IEEE 14 Networks

k	$\mathcal{A} = 25\%$		$\mathcal{A} = 50\%$		$\mathcal{A} = 100\%$	
	Gas (%)	MW	Gas(%)	MW	Gas (%)	MW
1	29.39	13.52	29.39	13.52	29.39	13.52
2	47.30	21.90	50.39	23.19	50.39	23.21
3	54.79	21.88	75.07	31.25	75.07	31.25
4	59.73	23.64	81.35	32.98	88.86	37.15
5	61.03	23.64	82.66	32.99	95.14	39.34
6	61.03	23.64	83.38	33.32	97.98	39.34
7	61.03	23.64	83.38	33.32	99.28	39.34
8	61.03	23.64	83.38	33.32	100.00	39.67

generation capacity varies for all cases. This highlights the importance of area restrictions. Communicating details on the allocation of the vulnerabilities is crucial for planning and operating the systems jointly. Fig. 3.4 shows an example of loss in capacity allocated to each of the generators in the system. Power generation vulnerabilities cannot be assessed properly if not considering the distribution of lost gas flow for all generators connected to the GN. Different distributions, depending on the gas impacted area, impact power generation uniquely.

Fig. 3.5 shows the increase in gas shed as k increases. The spread between the two $\mathcal{A} = 25\%$ shows the variability in outcome when the epicenter changes. In future work, through multiple iterations, for example doing Monte Carlo simulations, we can get the mean and variance of the loss of load as k increases.

Restricting the original N - k analysis to a subset of components enforces load shed for all gas consumers, regardless of being in the bulk distribution system or gas-fired generators, without minimizing gas shed to the PN. Furthermore, the higher the values of k , the greater

Table 3.7: Gas Shed and Lost Power Capacity per Damaged Area Size For NE-IEEE 36 Networks

k	$\mathcal{A} = 25\%$		$\mathcal{A} = 50\%$		$\mathcal{A} = 100\%$	
	Gas (%)	MW	Gas(%)	MW	Gas (%)	MW
1	24.29	651.24	24.29	429.35	24.29	651.24
2	39.09	678.26	39.08	686.95	39.09	531.22
3	47.29	866.33	47.26	960.93	47.34	952.97

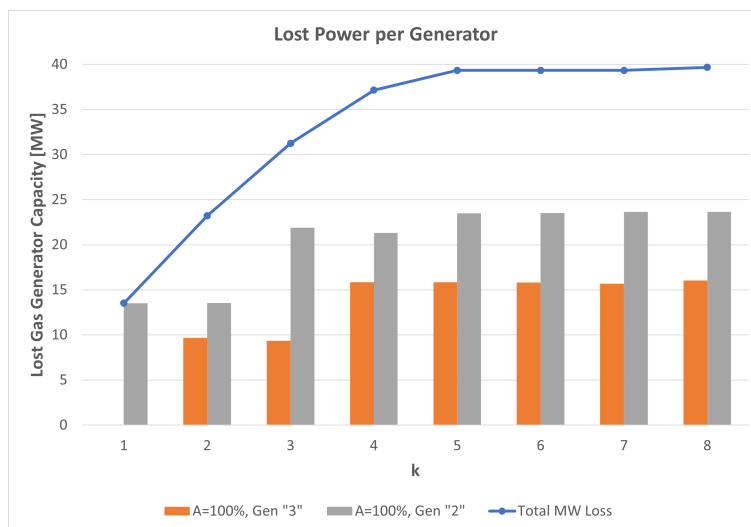


Figure 3.4: Power Capacity Lost per generator for $\mathcal{A} = 100$. IEEE-14 case system

the difference in expected loss of gas. Identification of vulnerabilities, through worst case scenario identification methods cannot be evaluated disjointedly since the effect of correlated failures is important to consider.

3.5.4 Probabilistic Assessment of Natural Disaster

The previous two projects identified deficits in natural gas for power generators within a restricted physical space under extreme events. The results shown in Figure 3.5 represent

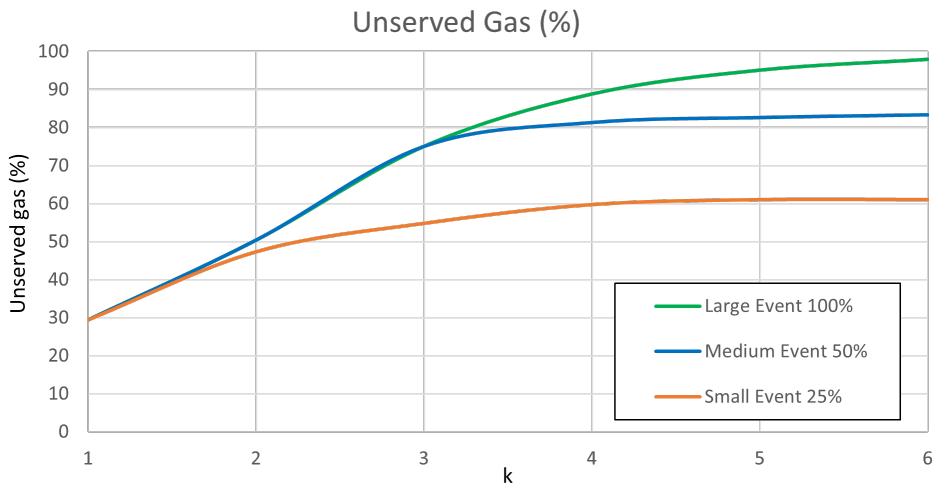


Figure 3.5: Gas not served for $\mathcal{A} =$ large, medium and small event magnitudes

different magnitudes of HILP events coupled with an $N-k$ deterministic contingency analysis. Each deterministic sub-problem detailed in prior work was weighted by magnitude. The restricted the set of possible outage failures to those above a certain threshold of fault correlation was set by a data matrix that set spatial proximity from each components to the rest of the network.

3.6 Summary

This research presented the first systematic algorithm to compute worst-case $N-k$ contingencies on natural gas pipeline networks by modeling relaxations of steady-state gas flow physics. The computational effectiveness of the algorithm, its scalability, and the potential use of such a tool to estimate the impact of a worst-case $N-k$ contingency on the bulk-electric system were shown through extensive computational experiments on case studies involving several widely available test networks. performing a joint $N-k$ interdiction analysis where a total of k components can be interdicted in either the power grid or gas pipeline system, where the modeling involves power flow and steady-state gas flow physics, respectively;

and planning resilient networks against Natural Hazards by understanding the importance of correlated failures [7]. Finally, compromise between theoretical worst-case scenario and a practical approach to restrict the attack and use the formulation as a tool for network expansion assessments.

Chapter 4

EVALUATION OF ROBUSTNESS STRATEGIES AGAINST EXTREME EVENTS

4.1 Motivation

The electrical grid is designed to meet demand during normal operation and even in the event of a contingency. To meet demand there are practices and protocols in place at every level of power system operation. System regulators oversee that all players are in compliance with such standards. With lessons learned through more than 100 years of experience operating the grid and navigating its challenges, we have optimized our systems through market regulations, economic dispatch, demand response programs, etc to minimize cost, maximize profit for stakeholders and meet demand. Yet there is still a trade off between optimizing and investing in maintenance and insurance policy in unforeseen circumstances. Investments on resilience are difficult to justify because the benefits are only tangible during an infrequent extreme event, nevertheless some strategies can also provide better reliability performance, which benefit is embedded in the operation design, while furthering resilience.

The pattern that we could rely upon to prepare for natural disasters is also changing due to climate change. The paradigms are changing and we need to adapt. Also, our electricity grid composition is also changing, specifically with the increasing penetration of renewables, enabling technology in power electronics for intelligent switching and overall lessons learned that enable our grid designs to address modern threats. Grid edge technologies have developed in recent years as the leading solution towards a decentralized, net zero power grid. High penetration of DERs like solar or Small generators on the distribution network are providing services in the effort to decarbonize the grid and also add flexibility. Besides these services, there is an upside to DERs in aiding resilience during a contingency. On the other

hand, the current grid infrastructure is ageing. All infrastructure assets have a life cycle, periodic maintenance requirements and constant monitoring. There needs to be investment to keep functionality and health of grids.

The focus of this work is to compare different grid modernization strategies in order to improve resilience [15], specifically address the pre-event phase of the resilience trapezoid [10] which determines the robustness of a grid during an attack. The ability to absorb and withstand an attack by measuring the loss of load expectation (LOLE) delivered after an event compared to the normal operating point prior to the attack. **We want to determine the best enhancement to a given distribution network, within a portfolio of investments, that when subjected to a high impact low probability (HILP) event, it minimizes LOLE and investment cost.**

4.2 Literature Review

Hardening is regular and common practice employed to upgrade existing power system assets like poles and lines to maintain reliability metrics, e.g. unserved load, at a high standard. Yet the benefit of hardening seems diminished under extreme circumstances. On the other hand, distributed resources are costly and require optimization in planning to reap the benefits but can add flexibility to supply load during an outage as talked about in chapter 2.

A resilience-oriented design technique to protect distribution grids against high-impact but low-probability extreme weather events is found in [39]. The problem is formulated as a two-stage stochastic mixed integer problem. The first stage is to make pre-event decisions like hardening existing distribution lines and deploying back-up distributed generators and automatic switches. The second stage evaluates the system operation cost during a realized extreme weather event and repair cost after the event. A novel modeling strategy is proposed to deal with the decision-dependent uncertainty of distribution line damage status, which is affected by the first-stage hardening decisions. As both stages have binary variables, a modified and computationally efficient progressive hedging algorithm with scenario

bundling is introduced. The algorithm performance is evaluated by calculating lower bounds of solutions.

Along with analysis, operation and execution strategies, Bie and Lin in [11] define the concepts and metrics for power system evaluation with hardening strategies and smart grid technologies that help increase system resilience. The adopted approach is through load restoration based on smart distribution technology. The methodology implemented can also be applied to recover after natural disasters, not only in preventive actions. The model proposed uses distributed generators (DGs) in islanding mode with optimal reconfiguration by simultaneously optimizing DG islanding usage with minimal load shedding in a MISOCP formulation.

Regarding tools that can help with decision making, [17] proposes an integrated solution: a distribution system restoration decision support tool designed by leveraging resources developed for grid modernization. There is a complete analysis on the flaws that current practices have when restoring after extreme weather events. Then, the proposal is to use grid modernization efforts to benefit distribution system restoration and in junction with a decision support tool better achieve the goal. The results shown are improving situational awareness of the system damage status and facilitating survive-ability for customers. Also, optimal and efficient allocation of repair crews and resources, the expediting of the restoration process, and the reduction of outage duration for customers, in response to severe blackouts due to extreme weather hazards.

Multi-stage restoration strategy is analyzed in [54] where they consider the uncertainty of outage duration to solve the service restoration problem in distribution systems. Furthermore, also proposed is a restoration index defined in terms of (i) priority of the load restored, (ii) number of switching operations, and (iii) estimated likelihood of the restoration solution to assist the utility in enhanced decision-making. Service restoration is formulated as a single objective optimisation problem considering the maximizing of the restoration index as the only objective. A decentralised multi-agent system method is developed to solve the service restoration problem considering controlled islanding of distributed generators. The

uncertainty of outage duration is estimated using the maximum entropy principle-based on the cause of the fault.

Finally, the literature spreads over many other different methods for restoration including PV solutions with microgrids [48], mobile power sources, including electric vehicle fleets, truck-mounted mobile energy storage systems and mobile emergency generators [36], electric vehicles as distributed energy resources [62] and optimized battery sizing for extreme events [26]. Load shedding is also a technique for restoration, but is limited in a situation of complete network devastation.

4.3 Proposed Method

Our framework is a simulation based approach to evaluate resilience against high wind speeds. Wind characterization curves are focused on the tail end of a Rayleigh distribution in order to properly evaluate the HILP events on resilience metrics. Secondly, fragility curves against wind speed for grid components are developed from historical data [18] of wind speed measurements correlated to component failures in Chile. The proposition is to use a sequential Monte Carlo simulation to address the stochastic elements of the model. The previous formulation is shown schematically in Figure 4.1.

A generic example is depicted in Fig. 4.2, where random faults (red lightning strikes), hardened lines (red dotted) and installed distributed resources (green circles) in a distribution network represent a possibility of actions from a wide range of portfolio options.

The following subsections will present the detail of each component in the framework.

Fragility Curves

Fragility curves describe the likelihood of a component failing when under endogenous or exogenous strain. We used fragility curves obtained from real events in Santiago in Chile. Wind speed measurements at local meteorological sites shown in Fig. 4.3 are used to create an average of wind profile present in the distribution network. Component faults were confirmed

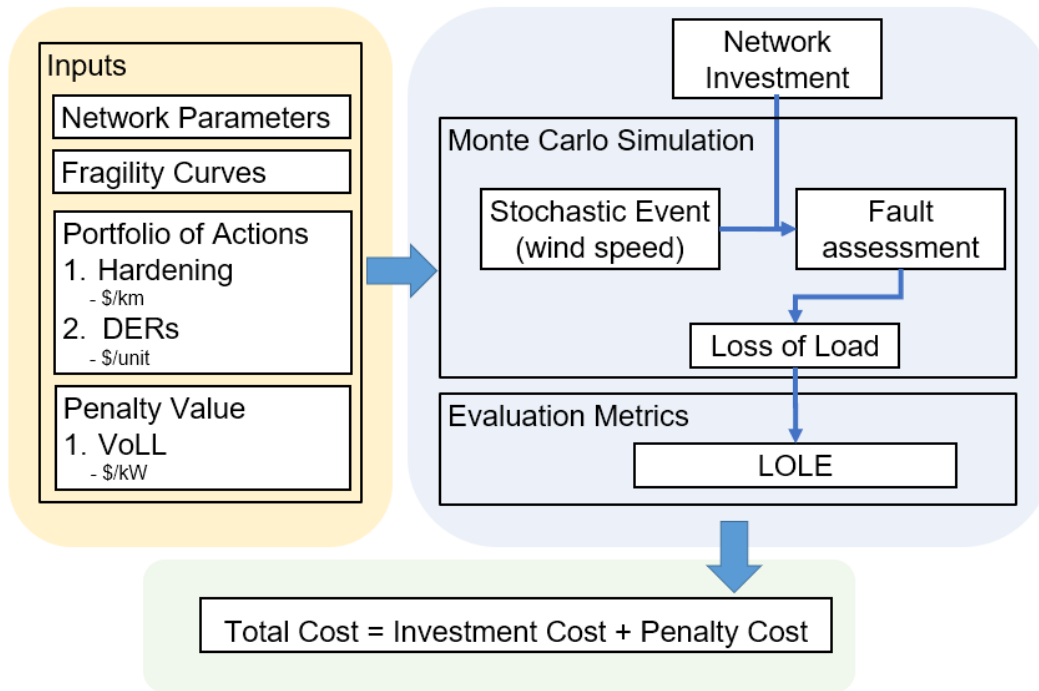


Figure 4.1: Resilience Evaluation Model

by utilities and then correlated to the speed at which a determined component failed in [18]. The interpolation resulted in equation (4.1).

The probability of failure given a line segment length is

$$P(l, \omega) = a \cdot l \cdot \omega^b \quad (4.1)$$

where l is the length of the line segment, a and b are constants obtain from data interpolation with values of 0.009194 and 2.354 respectively. ω is wind speed in km/h, depicted in figure 4.4 for 3 different lengths.

Event Characterization

We characterize a wind vector, e.i. frequency of wind intensity, that will attack the distribution grid infrastructure. This vector is characterized in two separate pools of intensity in

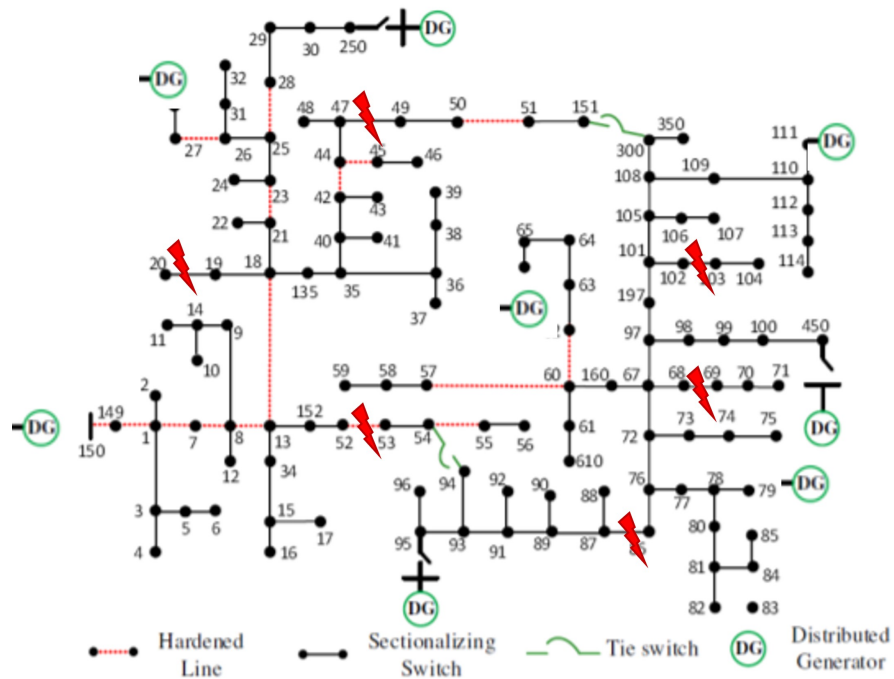


Figure 4.2: Distribution network with random faults, hardened lines and installed distributed resources.

figure 4.5. For reliability metrics a median wind speed of $10\text{km}/\text{h}$ is used. For resilience based evaluation, we want to 'zoom' into the tail end, where wind speeds are higher but less frequent to have a complete representation of HILP events. The median speed for resilience is $60\text{km}/\text{h}$.

$$\omega = \sigma\sqrt{-2\ln r} \quad (4.2)$$

Equation(4.2) shows a Rayleigh distribution where σ corresponds to the median speed and $r = U(0, 1)$ is a uniform distribution.

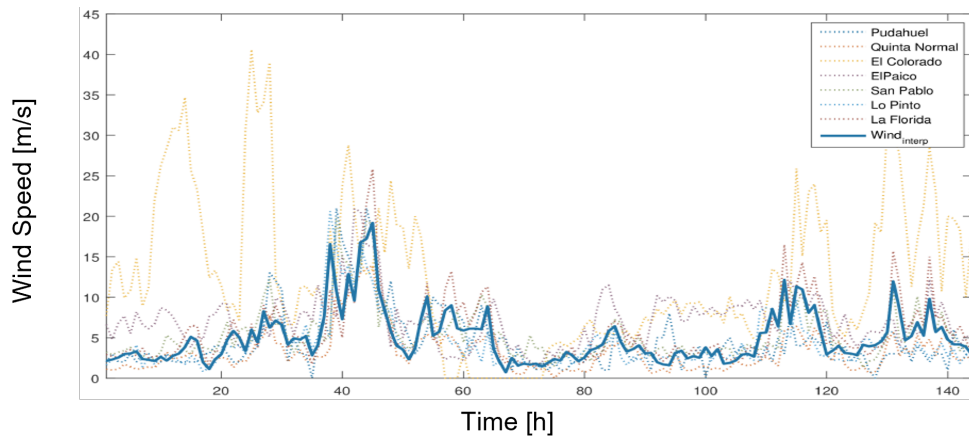


Figure 4.3: Measured wind speeds at 7 meteorological sites in Santiago, Chile

Fault Assessment

Each component will take on a binary status of *failed* or *not failed*. Utilizing a random coin toss for each component, if the result is greater than the probability of failure from Eq. 4.1, then the component does not fail, failure occurs otherwise as shown in Fig. 4.6.

Problem Formulation

Previous work [18] shows the evaluation of a IEEE-37 bus test system with 9 different enhancement options, including hardening (under-grounding lines), intelligent switching with micro grid forming capacity and connection to different feeders in a distribution grid. This initial evaluation of limited and thought-out portfolio is broadened by an optimization formulation that sweeps through granular combinations of hardening actions and DGs allocations such that the investment cost and LOLE is minimized.

Sets:

\mathcal{N} - Set of components in Network

Parameters:

D - DER cost [\$/unit]

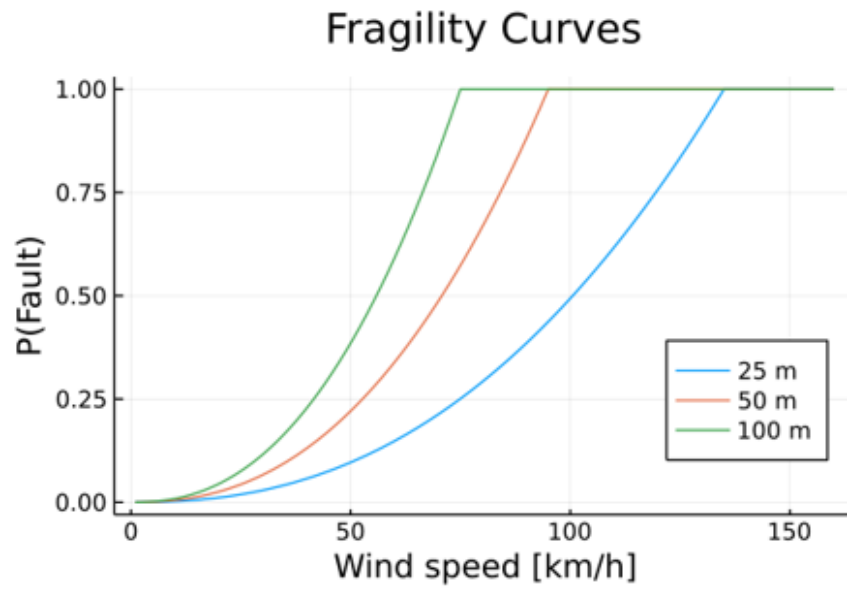


Figure 4.4: Line Fragility Curves for 3 line lengths.

H - Hardening cost [\$/km]

\mathcal{C} - resilience cost [\\$]

\mathcal{E}_L - Expected Load [kW]

\mathcal{LOL} - Loss of Load [kW]

Decision variables:

\mathcal{V}_{oLL} - Value of Lost Load [\$/kW]

d_i - DER allocation $\forall i \in \mathcal{N}$

h_i - Hardening action $\forall i \in \mathcal{N}$

The mathematical formation is as follows,

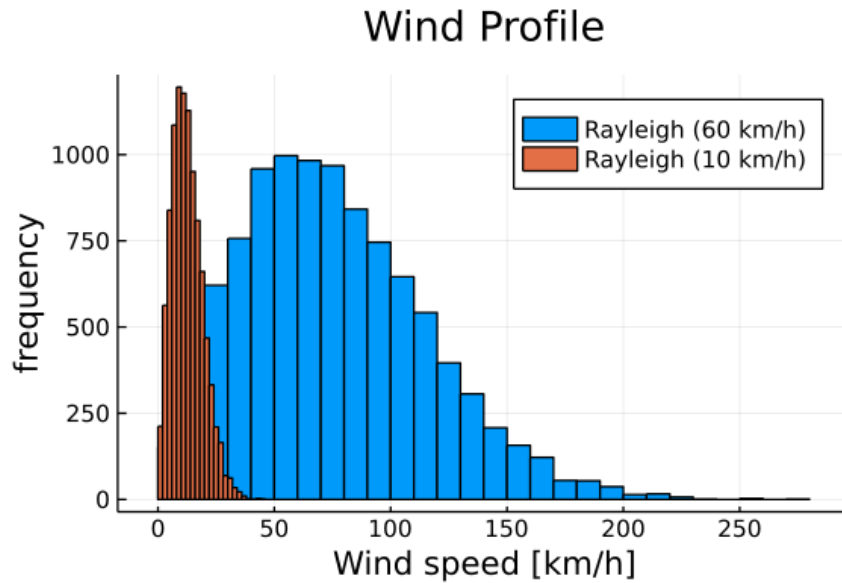


Figure 4.5: normal and extreme wind event characterization

$$\min C = D \sum_{i=1}^{\mathcal{N}} d_i + H \sum_{i=1}^{\mathcal{N}} h_i + VoLL \cdot LOLE \quad (4.3)$$

$$\text{subject to} \quad (4.4)$$

$$LOLE = \frac{LOL}{E_L} \cdot 100 \quad [\%] \quad (4.5)$$

$$d_i = \begin{cases} 1, & \text{if } DER = 1 \\ 0, & \text{otherwise} \end{cases} \quad (4.6)$$

$$h_i = \begin{cases} 1, & \text{if hardening} = 1 \\ 0, & \text{otherwise} \end{cases} \quad (4.7)$$

Simulation

Wind speed vectors and component failure assessment are incorporated into a Monte Carlo simulation to create scenarios with an algorithm that evaluates a complete portfolio of

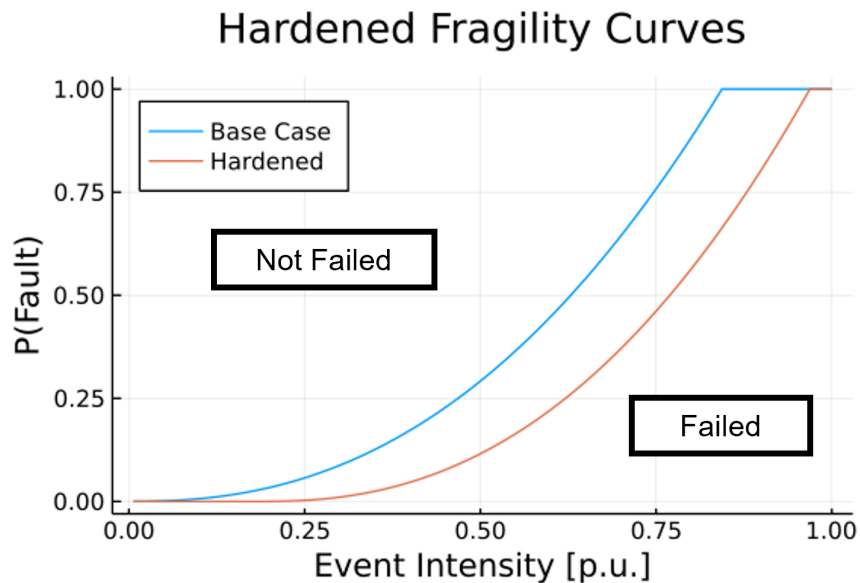


Figure 4.6: Binary component states for a base fragility curve (blue) and the hardened case (red).

robustness-aiding alternatives with a mix of hardening and DERs. Each action has an allocated investment cost. Each strategy is subjected to a variety of simulated natural disasters following the wind distribution and fragility curve models. The solution method is a two stage stochastic problem, where the first step is implementing deterministic resilience actions and then evaluating resilience metrics against hazards. A simplified schematic of the proposed solution is presented in algorithm 4.3.

Note all components from a network \mathcal{N} are assigned a probability of failure. If $h_i = 1$, the fragility curve utilized will be the hardened curve $P_h(\omega, l)$. If $h_i = 0$ then $P_0(\omega, l)$, Finally, if $d_i = 1$, then $P(\omega, l) = 0$.

4.4 Simulation Results

We implemented our formulation in the IEEE 37 bus test case. The following Monte Carlo simulations provides a 95 % confidence interval for LOLE with over 10000 iterations.

Algorithm 4

Input: Wind speed vector

Input: Fragility curves

Input: Network topology

Output: Investment Cost and LOLE

- 1: **for** 10000 iterations, **do** ▷ 95% confidence
 - 2: Compute ω
 - 3: Compute random vector $P(x_i) = U(0, 1) \quad \forall i \in \mathcal{N}$
 - 4: **if** $P(\omega, l) > P(x_i)$ **then** $x_i = 1$
 - 5: **else** $x_i = 0$
 - 6: **if** $x_i = 1$ **then** include component in LOL calculation
 - 7: **else** component failed
 - 8: Calculate LOL
 - 9: Calculate LOLE
 - 10: Calculate investment cost
-

Figure 4.7 shows various investment actions decomposed by their investment in Hardening against DERs. The circle size represents the LOLE if such investment option were to be implemented.

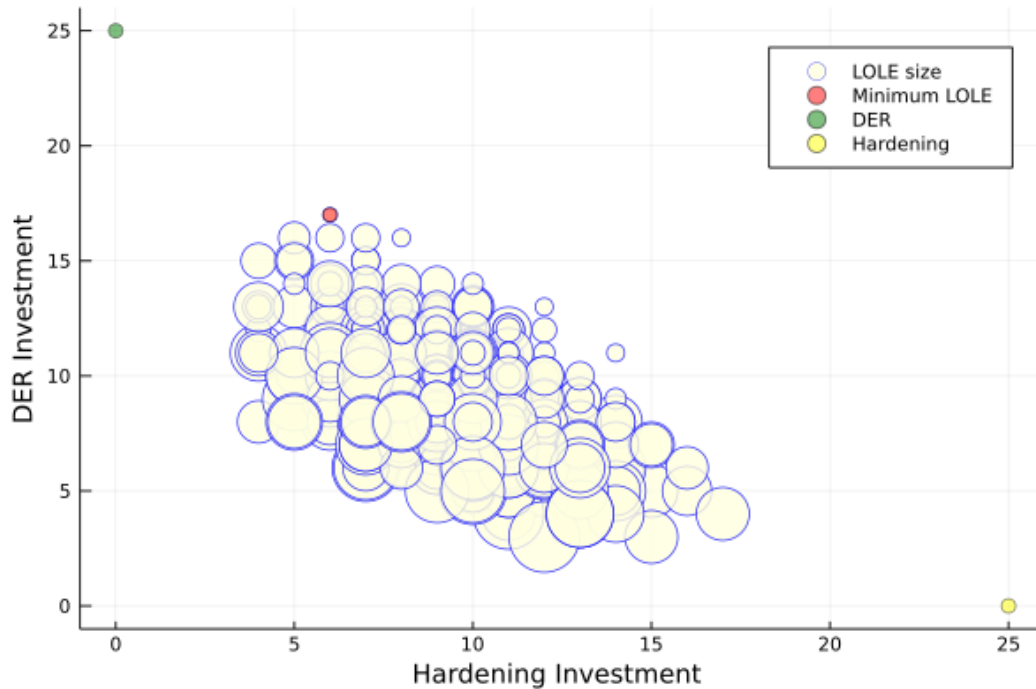


Figure 4.7: Investment decomposition for Harding and DERs for different portfolio strategies. Size of the circles represents the LOLE.

Figures 4.8 and 4.9 are the expected loss of load in return for the investment adopted given different VoLL values.

4.5 Summary

This study shows a map of portfolio strategies and how they fair against wind speeds. The presented case study is a proof of concept and would require further development in the underlying assumptions such as topology of network and computational efficiency for larger networks. We show the trade-offs of investment in hardening of lines and poles against

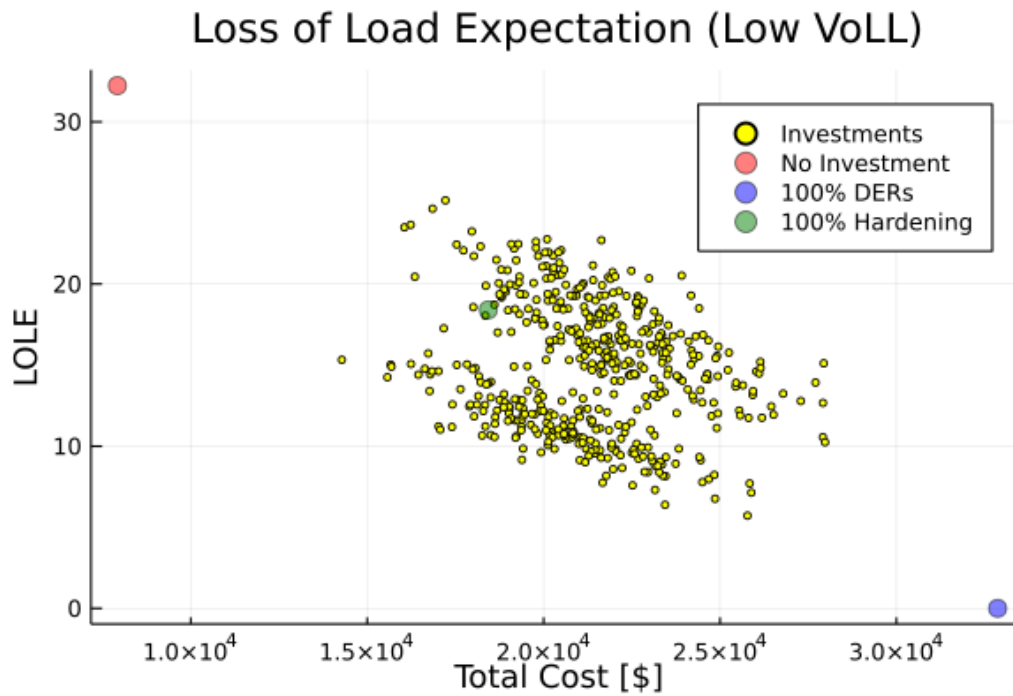


Figure 4.8: LOLE vs Investment Cost with Low VoLL

adding distributed generation capacity in the system to mitigate loss of load in robustness. This framework expands the previous assessment made in [18] where only a few options are considered within their portfolio, although the metrics used rely on energy not served (ENS), since restoration is also taken into account. The solution still has many assumptions to address to achieve a feasible implementation, such as a limited investment cost, policy restrictions to harden lines or invest in switching for DERs and most importantly, real assessment of VoLL.

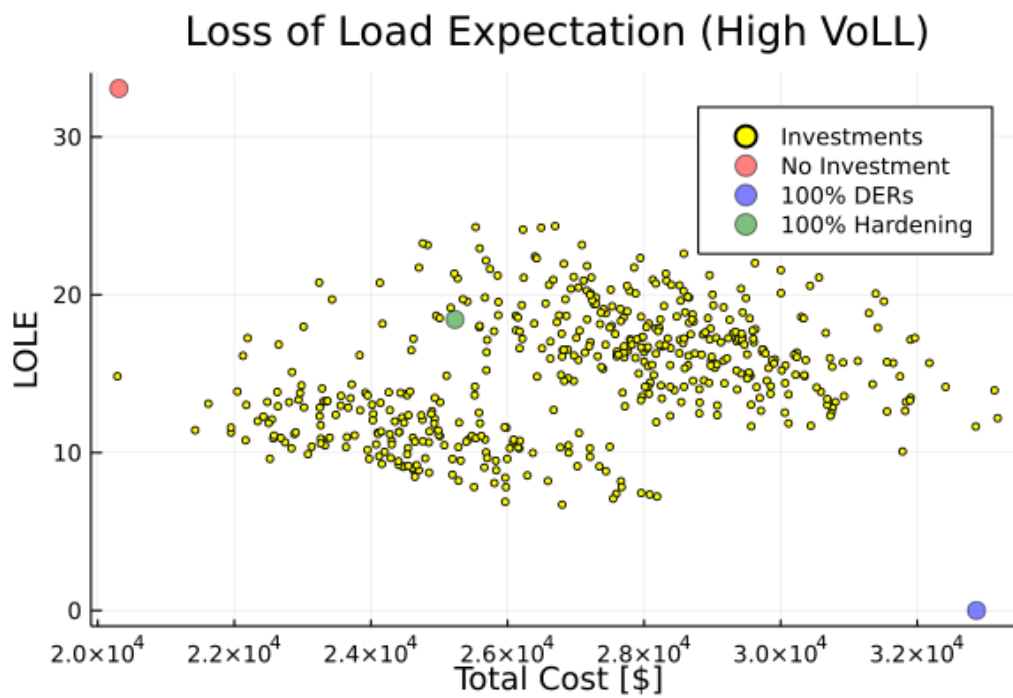


Figure 4.9: LOLE vs Investment Cost with High VoLL

Chapter 5

CONCLUSION

5.1 Key Results

The goal of my research was to analyze power systems resilience withing a framework of multiple infrastructures to better address vulnerabilities against natural disasters and reduce overall harm to operation.

In chapter 2, we used a case study to exemplify the importance of setting critical load as a driver for restoration. We used optimization tools to properly size PV-Battery systems that helped people dependent on electricity for their medical needs survive through a long term outage (months). Under the extreme circumstances of complete grid devastation, distributed resources such as small diesel generators and PV-Battery systems are the most common options for rural customers to survive during a hurricane; PV-battery systems, in addition, have the flexibility to operate in both islanded mode and connected to the grid to aid customers throughout normal grid operation and outages. This work has been published in IEEE Power and Energy Magazine [32] and Disaster Medicine and Public Health Preparedness Journal [61].

In chapter 3, we showed a systematic algorithm to compute worst case N-k contingencies on natural gas pipeline networks. We demonstrated its computational scalability and thus a helpful tool in evaluating and designing future infrastructure assets. Secondly we identified and modeled key vulnerabilities between natural gas infrastructure and the electric grid under natural disaster events. Lastly, we assessed a probabilistic model of HILP events coupled with a deterministic approach of worst-case scenarios. This work was presented at PSCC 2020 and published in Electric Power Systems Research Journal [1].and presented in IEEE-General Meeting 2022.

In chapter 4, we evaluated different hardening and robustness strategies under the presence of natural disasters. We used a Monte Carlo simulation for evaluating a complete spectrum of combinations between hardening and distributed energy resources as well as different hazard strengths for wind speeds. This work was presented as a student poster at the Fifth Workshop on Autonomous Energy Systems at NREL in July 2022.

In general, resilience investment is crucial as we navigate unprecedented events. Climate change is shifting planning and operation paradigms constantly and we need to adapt swiftly in order to maintain our way of life. Policy and market models need to find ways in allocating value to investment on resilience a priority and worthwhile to stakeholders.

5.2 Suggestions for Future Research

Resourcefulness, robustness and adaptability outlined in the previous thesis contribute to a small part of resilience in power systems. From thoughtful conversations with experts in the field and along other literature the next few suggestions are proposed:

- Implement a pipeline of lessons learned during emergencies in order to proactively address future disasters. Comparing isolated events to one another could be complex, given location, community, magnitude and infrastructure, nevertheless, standardizing response teams, planning and operations strategies across the board could help reduce cost in implementing solutions.
- Joint Gas-Power network extension to a transient gas flow model to identify $N-k$ contingencies that occur over time.
- Build-in energy transition objectives to a decarbonized grid and buildings by re-utilizing natural gas infrastructure to inject renewable alternatives such as renewable hydrogen.
- Incorporate VoLL quantification methods in optimization models.

- Create multi-objectives, including resilience and equity as main pillars in planning and operation through market design, economic incentives and policy.

Finally I would like to acknowledge all my collaborators and mentors throughout my studies leading up to this thesis.

BIBLIOGRAPHY

- [1] Mareldi Ahumada-Paras, Kaarthik Sundar, Russell Bent, and Anatoly Zlotnik. N-k interdiction modeling for natural gas networks. *Electric Power Systems Research*, 190:106725, 2021.
- [2] Rogelio E Alvarez. *Interdicting electrical power grids*. PhD thesis, Naval Postgraduate School, Monterey, California, 2004.
- [3] M. Amin. North america’s electricity infrastructure: are we ready for more perfect storms? *IEEE Security Privacy*, 1(5):19–25, Sep. 2003.
- [4] M. Amin. Challenges in reliability, security, efficiency, and resilience of energy infrastructure: Toward smart self-healing electric power grid. In *2008 IEEE Power and Energy Society General Meeting - Conversion and Delivery of Electrical Energy in the 21st Century*, pages 1–5, July 2008.
- [5] A. Ashok, M. Govindarasu, and J. Wang. Cyber-physical attack-resilient wide-area monitoring, protection, and control for the power grid. *Proceedings of the IEEE*, 105(7):1389–1407, July 2017.
- [6] Luis Ayala and Seth Blumsack. The braess paradox and its impact on natural-gas-network performance. *Oil and Gas Facilities*, 2(3):52–64, June 2013.
- [7] Javiera Barrera, Pauline Beaupuits, Eduardo Moreno, Rodrigo Moreno, and Francisco D. Muñoz. Planning resilient networks against natural hazards: Understanding the importance of correlated failures and the value of flexible transmission assets. *Electric Power Systems Research*, 197:107280, 2021.
- [8] Battery University. How to prolong lead-acid batteries, 2018.
- [9] R. Bent, S. Blumsack, P. Van Hentenryck, C. Borraz-Sánchez, and M. Shahriari. Joint electricity and natural gas transmission planning with endogenous market feedbacks. *IEEE Transactions on Power Systems*, 33(6):6397–6409, November 2018.
- [10] Alfred R Berkeley III, Mike Wallace, and Constellation COO. A framework for establishing critical infrastructure resilience goals. *National Infrastructure Advisory Council*, 2010.

- [11] Z. Bie, Y. Lin, G. Li, and F. Li. Battling the extreme: A study on the power system resilience. *Proceedings of the IEEE*, 105(7):1253–1266, July 2017.
- [12] Daniel Bienstock and Abhinav Verma. The n - k problem in power grids: New models, formulations, and numerical experiments. *SIAM Journal on Optimization*, 20(5):2352–2380, 2010.
- [13] Conrado Borraz-Sánchez, Russell Bent, Scott Backhaus, Hassan Hijazi, and Pascal Van Hentenryck. Convex relaxations for gas expansion planning. *INFORMS Journal on Computing*, 28(4):645–656, 2016.
- [14] Gerald Brown, Matthew Carlyle, Javier Salmerón, and Kevin Wood. Defending critical infrastructure. *Interfaces*, 36(6):530–544, 2006.
- [15] S. Chanda, A. K. Srivastava, M. U. Mohanpurkar, and R. Hovsopian. Quantifying power distribution system resiliency using code-based metric. *IEEE Transactions on Industry Applications*, 54(4):3676–3686, July 2018.
- [16] H. Chao and R. J. Ringlee. Analytical challenges in reliability and resiliency modeling. In *2018 IEEE International Conference on Probabilistic Methods Applied to Power Systems (PMAPS)*, pages 1–5, June 2018.
- [17] C. Chen, J. Wang, and D. Ton. Modernizing distribution system restoration to achieve grid resiliency against extreme weather events: An integrated solution. *Proceedings of the IEEE*, 105(7):1267–1288, July 2017.
- [18] A. Chávez Enríquez. Portafolios tecnológicos para el diseño confiable y resiliente de redes de distribución utilizando flujos lineales ac. Master’s thesis, University of Chile, 2020.
- [19] Carleton Coffrin, Russell Bent, Byron Tasseff, Kaarthik Sundar, and Scott Backhaus. Relaxations of AC Maximal Load Delivery for Severe Contingency Analysis. *IEEE Transactions on Power Systems*, 34(2):1450–1458, March 2019.
- [20] Carleton Coffrin, Russell Bent, Kaarthik Sundar, Yeesian Ng, and Miles Lubin. Powermodels.jl: An open-source framework for exploring power flow formulations. In *2018 Power Systems Computation Conference (PSCC)*, pages 1–8, June 2018.
- [21] J.A. Cohn. *The Grid: Biography of an American Technology*. The MIT Press. MIT Press, 2018.

- [22] Hao Cong, Yang He, Xu Wang, and Chuanwen Jiang. Robust optimization for improving resilience of integrated energy systems with electricity and natural gas infrastructures. *Journal of Modern Power Systems and Clean Energy*, 6(5):1066–1078, September 2018.
- [23] T D. O’Rourke and Thomas R. Briggs. Critical infrastructure, interdependencies, and resilience. *The Bridge*, 37, 01 2007.
- [24] Daniel de Wolf and Yves Smeers. Optimal dimensioning of pipe networks with application to gas transmission networks. *Operations Research*, 44(4):596–608, 1996.
- [25] Vaibhav Donde, Vanessa López, Bernard Lesieutre, Ali Pinar, Chao Yang, and Juan Meza. Severe multiple contingency screening in electric power systems. *IEEE Transactions on Power Systems*, 23(2):406–417, 2008.
- [26] J. Dong, L. Zhu, Y. Su, Y. Ma, Y. Liu, F. Wang, L. M. Tolbert, J. Glass, and L. Bruce. Battery and backup generator sizing for a resilient microgrid under stochastic extreme events. *IET Generation, Transmission Distribution*, 12(20):4443–4450, 2018.
- [27] Iain Dunning, Joey Huchette, and Miles Lubin. Jump: A modeling language for mathematical optimization. *SIAM Review*, 59(2):295–320, 2017.
- [28] F. Robles. Puerto Rican Government Acknowledges Hurricane Death Toll of 1,427., August 2018.
- [29] F. Robles, K. Davis, S. Fink and S. Almukhtar. Official toll in Puerto Rico: 64. Actual deaths may be 1,052., December 2017.
- [30] Omar Jose Guerra Fernandez, Brian Sergi, Michael Craig, Kwabena Addo Pambour, Carlo Brancucci, Brian Hodge, and Rostand Tresor Sogwi. Electric power grid and natural gas network operations and coordination. *OSTI.gov*, 9 2020.
- [31] K. Anderson, K. Burman, T. Simpkins, E. Helson and L. Lisell. New York solar smart DG hub-resilient solar project: Economic and resiliency impact of PV and storage on New York critical infrastructure. Technical report, National Renewable Energy Laboratory (NREL) and City University of New York (CUNY), June 2016.
- [32] Chanaka Keerthisinghe, Mareldi Ahumada-Paras, Lilo D. Pozzo, Daniel S. Kirschen, Hugo Pontes, Wesley K. Tatum, and Marvi A. Matos. Pv-battery systems for critical loads during emergencies: A case study from puerto rico after hurricane maria. *IEEE Power and Energy Magazine*, 17(1):82–92, 2019.

- [33] Taedong Kim, Stephen J Wright, Daniel Bienstock, and Sean Harnett. Analyzing vulnerability of power systems with continuous optimization formulations. *IEEE Transactions on Network Science and Engineering*, 3(3):132–146, 2016.
- [34] Kishore, Nishant and Marqués, Domingo and Mahmud, Ayesha and Kiang, Mathew V. and Rodriguez, Irmay and Fuller, Arlan and Ebner, Peggy and Sorensen, Cecilia and Racy, Fabio and Lemery, Jay and Maas, Leslie and Leaning, Jennifer and Irizarry, Rafael A. and Balsari, Satchit and Buckee, Caroline O. Mortality in puerto rico after hurricane maria. *New England Journal of Medicine*, 379(2):162–170, 2018. PMID: 29809109.
- [35] L. Santiago, C. E. Shoichet and J. Kravarik. Puerto Rico’s new Hurricane Maria death toll is 46 times higher than the government’s previous count, August 2018.
- [36] S. Lei, C. Chen, H. Zhou, and Y. Hou. Routing and scheduling of mobile power sources for distribution system resilience enhancement. *IEEE Transactions on Smart Grid*, pages 1–1, 2018.
- [37] Tao Li, Mircea Eremia, and Mohammad Shahidehpour. Interdependency of natural gas network and power system security. *IEEE Transactions on Power Systems*, 23(4):1817–1824, 2008.
- [38] Cristin Lyons and Greg Litra. Gas-power interdependence: Knock-on effects of the das to gas. <http://www.scottmadden.com/insight/gaspower-interdependence/>, 2013.
- [39] S. Ma, L. Su, Z. Wang, F. Qiu, and G. Guo. Resilience enhancement of distribution grids against extreme weather events. *IEEE Transactions on Power Systems*, 33(5):4842–4853, Sep. 2018.
- [40] Saeed D. Manshadi and Mohammad E. Khodayar. Resilient operation of multiple energy carrier microgrids. *IEEE Transactions on Smart Grid*, 6(5):2283–2292, 2015.
- [41] Garth P McCormick. Computability of global solutions to factorable nonconvex programs: Part i—convex underestimating problems. *Mathematical programming*, 10(1):147–175, 1976.
- [42] W.K.C. Morgan, R.B. Reger, and D.M. Tucker. Health effects of diesel emissions. *The Annals of Occupational Hygiene*, 41(6):643 – 658, 1997.
- [43] Alexis L Motto, José M Arroyo, and Francisco D Galiana. A mixed-integer LP procedure for the analysis of electric grid security under disruptive threat. *IEEE Transactions on Power Systems*, 20(3):1357–1365, 2005.

- [44] National Renewable Energy Laboratory (NREL). PV Watts Calculator, 2018.
- [45] Office of Cybersecurity, Energy Security, and Emergency Response, U.S. Department of Energy. Hurricanes Nate, Maria, Irma, and Harvey Situation Reports, April 2018.
- [46] Ali Pinar, Juan Meza, Vaibhav Donde, and Bernard Lesieutre. Optimization strategies for the vulnerability analysis of the electric power grid. *SIAM Journal on Optimization*, 20(4):1786–1810, 2010.
- [47] Shiva Poudel, Anamika Dubey, and Anjan Bose. Risk-based probabilistic quantification of power distribution system operational resilience. *IEEE Systems Journal*, 14(3):3506–3517, 2020.
- [48] S. Qazi and W. Young. Disaster relief management and resilience using photovoltaic energy. In *2014 International Conference on Collaboration Technologies and Systems (CTS)*, pages 628–632, May 2014.
- [49] Z. Qiao, L. Jia, W. Zhao, Q. Guo, H. Sun, and P. Zhang. Influence of n-1 contingency in natural gas system on power system. In *2017 IEEE Conference on Energy Internet and Energy System Integration (EI2)*, pages 1–5, November 2017.
- [50] Steven M Rinaldi, James P Peerenboom, and Terrence K Kelly. Identifying, understanding, and analyzing critical infrastructure interdependencies. *IEEE Control Systems*, 21(6):11–25, 2001.
- [51] Javier Salmeron, Kevin Wood, and Ross Baldick. Analysis of electric grid security under terrorist threat. *IEEE Transactions on Power Systems*, 19(2):905–912, 2004.
- [52] Javier Salmeron, Kevin Wood, and Ross Baldick. Worst-case interdiction analysis of large-scale electric power grids. *IEEE Transactions on Power Systems*, 24(1):96–104, 2009.
- [53] Martin Schmidt, Denis Aßmann, Robert Burlacu, Jesco Humpola, Imke Joormann, Nikolaos Kanelakis, Thorsten Koch, Djamal Oucherif, Marc E Pfetsch, Lars Schewe, et al. Gaslib – A library of gas network instances. *Data*, 2(4):40, 2017.
- [54] A. Sharma, A. Trivedi, and D. Srinivasan. Multi-stage restoration strategy for service restoration in distribution systems considering outage duration uncertainty. *IET Generation, Transmission Distribution*, 12(19):4319–4326, 2018.
- [55] Huai Su, Enrico Zio, Jinjun Zhang, and Xueyi Li. A systematic framework of vulnerability analysis of a natural gas pipeline network. *Reliability Engineering and System Safety*, 175:79–91, 2018.

- [56] Kaarthik Sundar, Carleton Coffrin, Harsha Nagarajan, and Russell Bent. Probabilistic N - k failure-identification for power systems. *Networks*, 71(3):302–321, 2018.
- [57] Kaarthik Sundar, Sidhant Misra, Russell Bent, and Feng Pan. Spatial and topological interdiction for transmission systems. *arXiv preprint arXiv:1904.08330*, 2019.
- [58] Kaarthik Sundar and Anatoly Zlotnik. State and parameter estimation for natural gas pipeline networks using transient state data. *IEEE Transactions on Control Systems Technology*, 27(5):2110–2124, 2018.
- [59] A. Sydbom, A. Blomberg, S. Parnia, N. Stenfors, T. Sandström, and S-E. Dahlén. Health effects of diesel exhaust emissions. *European Respiratory Journal*, 17(4):733–746, 2001.
- [60] A.R.D. Thorley and C.H. Tiley. Unsteady and transient flow of compressible fluids in pipelines’: a review of theoretical and some experimental studies. *International Journal of Heat and Fluid Flow*, 8(1):3–15, 1987.
- [61] Gabriella A. Tosado, Marvi Matos, Mareldi Ahumada-Paras, Michael K. Chapko, and Lilo D. Pozzo. Evaluation of solar-powered battery systems for individuals using electricity-dependent medical devices in puerto rico following hurricane maria. *Disaster Medicine and Public Health Preparedness*, page 1–4, 2021.
- [62] T. S. Ustun, U. Cali, and M. C. Kisacikoglu. Energizing microgrids with electric vehicles during emergencies — natural disasters, sabotage and warfare. In *2015 IEEE International Telecommunications Energy Conference (INTELEC)*, pages 1–6, Oct 2015.
- [63] S. S. M. Venkata and N. Hatziargyriou. Grid resilience: Elasticity is needed when facing catastrophes [guest editorial]. *IEEE Power and Energy Magazine*, 13(3):16–23, May 2015.
- [64] C. Wang, W. Wei, J. Wang, F. Liu, F. Qiu, C. M. Correa-Posada, and S. Mei. Robust defense strategy for gas–electric systems against malicious attacks. *IEEE Transactions on Power Systems*, 32(4):2953–2965, July 2017.
- [65] Y. Wang, C. Chen, J. Wang, and R. Baldick. Research on resilience of power systems under natural disasters—a review. *IEEE Transactions on Power Systems*, 31(2):1604–1613, March 2016.
- [66] Y. Wang, Y. Xu, J. He, C. Liu, K. P. Schneider, M. Hong, and D. T. Ton. Coordinating multiple sources for service restoration to enhance resilience of distribution systems. *IEEE Transactions on Smart Grid*, pages 1–1, 2019.

- [67] Z. Wang, M. Rahnamay-Naeini, J. M. Abreu, R. A. Shuvro, P. Das, A. A. Mammoli, N. Ghani, and M. M. Hayat. Impacts of operators' behavior on reliability of power grids during cascading failures. *IEEE Transactions on Power Systems*, 33(6):6013–6024, Nov 2018.
- [68] Z. Wang and J. Wang. Service restoration based on ami and networked mgs under extreme weather events. *IET Generation, Transmission Distribution*, 11(2):401–408, 2017.
- [69] R Kevin Wood. Bilevel network interdiction models: Formulations and solutions. *Wiley encyclopedia of operations research and management science*, 2010.
- [70] S. Xu, Y. Qian, and R. Q. Hu. On reliability of smart grid neighborhood area networks. *IEEE Access*, 3, 2015.
- [71] Y. Xu, C. Liu, K. P. Schneider, F. K. Tuffner, and D. T. Ton. Microgrids for service restoration to critical load in a resilient distribution system. *IEEE Transactions on Smart Grid*, 9(1):426–437, Jan 2018.
- [72] Y. Ieee guide for collecting, categorizing, and utilizing information related to electric power distribution interruption events. *IEEE Std 1782-2014*, pages 1–98, Aug 2014.

Appendix A

TOPIC GUIDE TO CONDUCT INTERVIEWS IN PUERTO RICO AFTER HURRICANE MARIA

Objectives: Quantify burden of lack of electricity on health of community

Subjects: Healthcare service providers and patients/family members

A.1 *Topic Guide: Patients*

Main Questions	Probes
Introductory/Cursory	
How did you experience the hurricane?	<ul style="list-style-type: none"> - Where were you? What happened? - Did you lose power? When? For how long? - How long was the storm? - Were you with someone or alone?
How did you prepare?	<ul style="list-style-type: none"> - When and for how long did you prepare? - Did you store extra supplies/medications? What kind? - Who helped you prepare?
How was your home affected by storm?	<ul style="list-style-type: none"> - Physical damage? Power outages? - Any supply shortages? - Running water? - Were you asked to relocate? Did you?

What kind of help did you receive after the storm?	<ul style="list-style-type: none"> - Describe any help you received. - From who? How frequently? - Did you request the help? - What is the current condition of your home?
Tell us how the lack of power affected your health.	<ul style="list-style-type: none"> - What type of medical devices do you use? Can we see them? - Do you use temperature sensitive medication?
What do you wish you had during the storm?	<ul style="list-style-type: none"> - And immediately after the storm?
How are your basic needs being met right now?	<ul style="list-style-type: none"> - Food? - Health? - Water? - Power?
Tell us more about you	<ul style="list-style-type: none"> - Where do you go for your healthcare? - How long does it usually take to get there? - How long did it take after the storm? - Have you seen your regular doctor since the hurricane?

Table A.1: Patients

Appendix B

RELAXATIONS FOR THE MGS PROBLEM

B.1 MINLP reformulation

To develop the relaxation for the MGS, we first reformulate the constraints in Eqs. (3.5b) – (3.5d) with binary flow direction variables y_e for each $e \in \mathcal{C} \cup \mathcal{P}$ [13]. Given a pipe or a compressor $e = (i, j) \in \mathcal{C} \cup \mathcal{P}$, y_e takes a value 1 if the mass flow is $f_e \geq 0$ and 0, otherwise. We remark that if $f_e \leq 0$, then gas is flowing from the node j to node i . Given these notations, Eq. (3.5b), for any $e = (i, j) \in \mathcal{P} : x_e = 0$ equivalently reformulated as

$$\gamma_e = \mathbf{w}_e f_e^2 \tag{B.1a}$$

$$\gamma_e \geq \pi_j - \pi_i + 2y_e(\underline{\pi}_i - \overline{\pi}_j) \tag{B.1b}$$

$$\gamma_e \geq \pi_i - \pi_j + 2(y_e - 1)(\overline{\pi}_i - \underline{\pi}_j) \tag{B.1c}$$

$$\gamma_e \leq \pi_j - \pi_i + 2y_e(\overline{\pi}_i - \underline{\pi}_j) \tag{B.1d}$$

$$\gamma_e \leq \pi_i - \pi_j + 2(y_e - 1)(\underline{\pi}_i - \overline{\pi}_j) \tag{B.1e}$$

$$- \mathbf{f}_e(1 - y_e) \leq f_e \leq \mathbf{f}_e y_e \tag{B.1f}$$

where, γ_e is an auxiliary variable for pipe e . Eqs. (B.1b) – (B.1e) are the McCormick envelopes [41] for the equation $\gamma_e = (2y_e - 1)(\pi_i - \pi_j)$. These envelopes result in an exact reformulation because it is the product of a variable that takes a value of one or negative one, $(2y_e - 1)$, with a continuous variable, $(\pi_i - \pi_j)$. Eq. (B.1f) bounds the mass flow on the pipe using the flow direction variable y_e . The only nonlinear constraint in the reformulation is Eq. (B.1a). As for the compressor constraints in Eqs. (3.5c) and (3.5d), a linear reformulation

of the constraints for every compressor $e = (i, j) \in \mathcal{C} : x_e = 0$ is given by:

$$y_e(\underline{\pi}_i - \overline{\pi}_j) \leq \pi_i - \pi_j \leq y_e(\overline{\pi}_i - \underline{\pi}_j) \quad (\text{B.2a})$$

$$\underline{\alpha}_e^2 \pi_i + (1 - y_e)(\underline{\pi}_j - \underline{\alpha}_e^2 \overline{\pi}_i) \leq \pi_j \quad (\text{B.2b})$$

$$\pi_j \leq \overline{\alpha}_e^2 \pi_i + (1 - y_e)(\overline{\pi}_j - \overline{\alpha}_e^2 \underline{\pi}_i) \quad (\text{B.2c})$$

$$- \mathbf{f}_e(1 - y_e) \leq f_e \leq \mathbf{f}_e y_e \quad (\text{B.2d})$$

where, Eqs. (B.2a) and (B.2b) – (B.2c) are disjunctive reformulations of Eqs. (3.5c) and (3.5d), respectively. Similar to pipes, Eq. (B.2d) bounds the mass flow on the compressor using the flow direction variable y_e . Using Eqs. in (B.1) and (B.2), the MINLP for the inner problem is then given by

$$\eta(\mathbf{x}) = \min \sum_{i \in \mathcal{N}} \lambda_i \mathbf{d}_i \text{ subject to: Eqs. (B.1), (B.2), (3.5e) – (3.5g).}$$

The MINLP reformulation of the MGS is still a difficult problem to solve to global optimality, even for small instances [13] and hence, the remainder of this section is focused on developing a MISOCP relaxation of the MINLP. The MISOCP is based on the formulation introduced in [13] and off-the-shelf commercial and open-source MISOCP solvers effectively solve the inner problem to optimality for a fixed \mathbf{x} .

Once an MISOCP relaxation is developed, off-the-shelf commercial and open-source MISOCP solvers can be put to effective use to solve the inner problem for a fixed \mathbf{x} to optimality.

B.2 MISOCP relaxation

The only nonlinear constraint in the MINLP reformulation is Eq. (B.1a). To obtain the MISOCP relaxation, we relax this constraint to

$$\gamma_e \geq \mathbf{w}_e f_e^2 \quad (\text{B.3})$$

which is a Second-Order Conic (SOC) constraint. Hence, the MISOCP relaxation of the inner-problem (MGS) is given by

$$\eta(\mathbf{x}) = \min \sum_{i \in \mathcal{N}} \lambda_i \mathbf{d}_i \text{ subject to:} \tag{B.4}$$

Eqs. (B.1b) – (B.1f), (B.3), (B.2), (3.5e) – (3.5g).

VITA

Mareldi Ahumada Parás is a Ph.D. candidate in the Department of Electrical and Computer Engineering at the University of Washington. Her research focuses on power system resilience, planning and impact of extreme events. In 2016 she was awarded a Fulbright Fellowship to pursue her graduate studies. Previously, she worked at General Electric Company as an Edison engineer and operability engineer from 2013 to 2016. While at GE, she worked on power turbines and remote diagnostics of existing fleet. Mareldi received her M.S.E degree at the University of Washington in 2020 and her B.S.E degree at Instituto Tecnológico de Monterrey, Campus Ciudad de México in 2013.